Research Article

Mediterranean Marine Science
Indexed in WoS (Web of Science, ISI Thomson) and SCOPUS
The journal is available on line at http://www.medit-mar-sc.net
DOI: http://dx.doi.org/10.12681/mms.16060

Comparative Performance Analysis of Different Wind Fields in the Southern and North-western Coastal Areas of the Black Sea

Recep Emre ÇAKMAK[1], Adem AKPINAR[1] and Gerbrant Ph. Van VLEDDER[2, 3]

[1] Uludağ University, Department of Civil Engineering, Gorukle Campus, Bursa, Turkey
[2] Delft University of Technology, Civil Engineering and Geosciences, The Netherlands
[3] VanVledder Consulting, Olst, The Netherlands

Corresponding author: ademakpinar@uludag.edu.tr

Handling Editor: Konstantinos TOPOUZELIS

Received: 6 March 2018; Accepted: 24 March 2019; Published on line: 8 July 2019

Abstract

This study determines the qualities of atmospheric wind field data in comparison with wind measurements at five locations along the Black Sea coast. For this purpose, four different wind fields were obtained from three different weather centers (NCEP, NASA, and ECMWF). Three of these are reanalyzed winds (Climate Forecast System Reanalysis CFSR, Modern-Era Retrospective-analysis for Research and Applications MERRA, ECMWF reanalyses ERA-Interim), and one is an operational dataset (ECMWF operational). Their performances were determined using the wind measurements from 2000 to 2014 at five coastal locations along the southern coastline of the Black Sea (Kumköy, Amasra, Sinop, Giresun, Hopa) and from 2006 to 2009 at the offshore location (Gloria) off the coast of Romania. The performances of these wind fields were determined based on statistical characteristics (mean, standard deviation and variation coefficient, etc.), the statistical error analysis for all data and for different wind speed intervals, the wind roses and the probability distributions. Additionally, long-term variations of the yearly error values (SI and bias) of wind speeds from wind data sources during 2000 - 2014 were discussed. Finally, it was concluded that the CFSR wids give the best performance at most stations. The ECMWF datasets yield better results along the western side but the CFSR wind fields have shown better performances along the eastern side of the Black Sea coast and at the Gloria offshore location.

Keywords: Wind speed; CFSR; MERRA; ERA-Interim; ECMWF Operational; Black sea.

Introduction

Weather forecast centers have developed various atmospheric flow prediction models that take several factors into account that affect these movements, which are experienced as wind. Each wind field is produced from a global model and the model results are disseminated with certain spatial and temporal resolutions. The wind fields covering the Black Sea are the subject of this study, as they are of interest for many engineering applications.

The wind climate is one of the most important factors in regard to coastal and marine activities. It is applied to a wide range of fields, such as sea transportation, wind power generation, wind wave modeling, coastal area management and planning, etc. Since it is not possible to find sufficient wave measurements, especially in long-term wave analyses, surface waves are produced by numerical modeling using long-term wind fields. In wind and wave climate studies, the data recorded at wind measuring locations that are closest to the study areas are usually used. The accuracy or suitability of such data depends on the type of measuring location, the distance to the study area and the temporal continuity of the data. Other important factors are the terrestrial properties imposed along the southern coasts of the Black Sea, where the wind measuring locations of the Turkish State Meteorological Service (TSMS) are located. It is known that there is an increasing orographic effect progression from the southwest toward the south-eastern part of the Black Sea. As in many ocean systems, the sea dynamics in the Black Sea are also influenced by the underwater topography. The water level gradients tend to be highest along regions with steep continental slopes. The western and north-western parts of the Black Sea are areas with low topographic gradients while the southern and eastern coasts are very steep (Stanev, 2005).

Winds affected by the orographic effects due to the presence of landforms have very different behavior compared to offshore winds. Considering the land topography of the area in which the wind is blowing, the presence of hills, valleys, cliffs, ridges and other height changes in the surface must be taken into account.

Coastal breezes are caused by the different heating and cooling patterns of the land and the sea. Since land heats up more rapidly than the sea during the day, the warm air onshore tends to rise, causing a drop in pressure. This draws in cooler, denser air from over the sea, causing an onshore breeze. At night, the process reverses with the land cooling down more quickly, where the air above it sinks and moves toward the lower pressure areas over the sea, causing an offshore breeze (Ponce de León & Orfila, 2013; Strahler & Strahler, 1992). Another feature that affects the wind resource is the Earth's surface. When the air moves against the land surface, its velocity is reduced due to friction with the ground. The magnitude of the frictional force is dependent on the characteristics of the particular surface in a location. These characteristics are summarized by the term roughness length, which is the theoretical height above a surface at which the effect of friction reduces the wind to zero velocity. Areas with a larger surface roughness value will cause a greater reduction in the wind velocity, which will theoretically reach zero at a certain height from the ground. It normally depends on the roughness of the sea-states, and the magnitude of the significant wave height. Water typically has a lower characteristic surface roughness length than might be found onshore and is often given a constant value of 0.0002 m (Cradden *et al.*, 2016). The influence of the transition from land to sea in terms of the thermal effects can have an impact on the wind conditions up to 100 km from the coastline (Lange *et al.*, 2004). For these reasons, data measurements on the land from the TSMS locations have to be converted to winds on the sea using empirical methods (Hsu, 1980; US Army, 2003, where a plot for the ratio of the wind speed over water to the wind speed over land as a function of the wind speed over land is given; Sifnioti *et al.* 2017). All these effects mean that the higher the network resolution of the measuring locations, the more accurate the results. Unfortunately, there is insufficient spatial coverage of the measurements in the study area. Due to these reasons, there is a need for wind data with high spatial, continuous and regular temporal resolution.

There have been many studies on wind data source benchmarking worldwide (for example Caires *et al.*, 2004; Chelton & Freilich, 2005; Ardhuin *et al.*, 2007; Lileo & Petrik, 2011; Jakobson *et al.*, 2012; Wang & Zeng, 2012; Jimenez *et al.*, 2012; Carvalho *et al.*, 2013; Alvarez *et al.*, 2014; Stopa & Cheung, 2014; Onea *et al.*, 2017; Onea & Rusu, 2018), but very few have been performed over the Black Sea (Arıkan, 1998; Onea & Rusu, 2014a; Onea & Rusu, 2014b; Van Vledder & Akpınar, 2015; Onea *et al.*, 2016), and in particular almost no studies have been conducted on the southern coastline. Arıkan (1998) benchmarked two different wind data and wave hindcasts that were estimated using these winds. He compared the results of the T213 (ECMWF) model with measurements (storms) of monitoring locations in the Black Sea. For this comparison, he evaluated the dominant directions of the storms and the highest observed wind velocities. This evaluation was made based on a linear regression and correlation analyses. He also made another comparison between the hourly wind records of some locations along the Black Sea coast and the digitized wind speeds from synoptic maps. The ECMWF data versus measurements at coastal locations, indicating underestimations, presented error values (RMSE and bias) of approximately 5 m/s. The low bias values resulted from the comparison between the synoptic data and the hourly measurements. The correlation value obtained here, however, did not exceed 0.3. A study by Onea & Rusu (2014b) examined the existing wind conditions in the Black Sea basin. They focused on the coastal environment of the south western Black Sea, where the analysis was conducted using 14-year long offshore measurements and two wind sources (ECMWF and NCEP) between 1999 and 2012. The abovementioned analysis was also conducted using satellite data. Based on these data sets, it was concluded that significant energetic wind conditions occurred mainly in the western part of the Black Sea. In general, a good agreement is observed between the measurements and the simulated data in terms of the complete spatial and seasonal wind changes in the area of interest. Van Vledder & Akpinar (2015) investigated the impact of different wind fields (NCEP CFSR, NASA MERRA, JRA-25, ECMWF Operational, ECMWF ERA-40 and ECMWF ERA-Interim), as well as the spatial and temporal resolution on the SWAN wave model for the Black Sea. The models' ability to predict normal and extreme wave conditions during 1996 was assessed. The assessment of the wind fields' quality was performed by comparing it with satellite data for only a one-year period. The wave data modeled using these wind fields were also compared with the measurements taken within the scope of the NATO TU-WAVES project and with satellite data. In these two studies, the performance of the wind fields was not directly compared against in situ wind measurements.

Ardhuin & Roland (2013) indicated that the primary input that affects the model's accuracy in wind-wave modeling is wind forcing, and the secondary factor is parameterization of the physical processes, i.e., the source terms. Therefore, this study aims to examine the performances of available wind fields against the measurements at coastal locations (Kumköy, Amasra, Sinop, Giresun, and Hopa) of TSMS located along the southern coastline of the Black Sea, as well as at one offshore location (Gloria) over the Black Sea (Fig 1). Unlike in previous works, the present study determines the accuracy of the new generation wind reanalysis data sets against wind measurements, focusing on the southern coast of the Black Sea. This significantly helps in making up for the shortcomings sighted in previous studies. The relationship between the measurements and hindcast data sets was first evaluated by using some statistical parameters, such as the minimum, mean, maximum, standard deviation, etc. By performing a simultaneous data analysis using temporally overlapping measurements and hindcast data, the statistical error indicators (mean absolute error MAE, root-mean-square error RMSE, scattering index SI, etc.), Pearson correlation and Willmott skill score were subsequently determined. The error analyses performed for all data were also done for the data at different speed ranges.

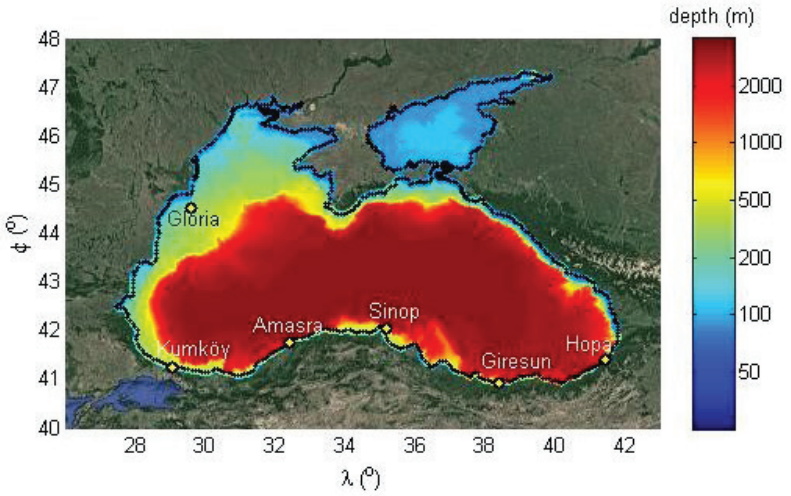

Fig. 1: The general view of the study area and the locations of the measurements.

Then, in order to make a directional assessment, the wind roses of the data sources was third, compared with those of the measurements. The probability distribution graphs were fourth, plotted to show the distribution of the wind speeds. These assessments were made by using the overlapping four-year data between 2004-2007 for the coastal locations and 2006-2009 for the Gloria offshore location. Finally, the yearly variations of the error values for the wind data sources against the measurements with respect to years were examined at each location.

Materials and Methods

Wind Fields

Over the last few years, productions of new generation reanalysis data sets, such as ERA-Interim from the ECMWF, the CFSR from the NCEP, and the MERRA from NASA, were launched. These new reanalysis data sets contributed to significant improvements in operational weather forecasting techniques (Carvalho *et al.,* 2014). ERA-Interim (Simmons *et al.,* 2007), equipped with data from later years from the ECMWF operational records, mostly makes use of observation sets obtained for ERA-40. The use of the four-dimensional data assimilation method for atmospheric analysis where the observations are sparse made the ERA-Interim project surpass the ERA-40 data (Dee *et al.*, 2011). Detailed information about the ERA-Interim reanalysis data sets can be found in Simmons *et al.* (2007). MERRA (Rienecker *et al.*, 2011) is a NASA reanalysis of the satellite ERA data. It was developed using the latest version of the Goddard Earth Observing System Data Assimilation System Version 5. Rienecker *et al.* (2011) mention that in MERRA the 3D-Var data assimilation algorithm is used based on the Statistical Interpolation (GSI) method and stated that the GSI method provided improvements relative to previous 3D-Var algorithms. The CFSR reanalysis built by the US NOAA NCEP has provided considerable improvements with an increase in the spatial resolution, in the use of satellite observations process, and in the use of sea temperature and salinity measurements for the NCEP-R2 reanalysis. It also had another significant improvement, which is being a single data set that is able to use atmosphere-ocean and ice-land binary models (Carvalho *et al.*, 2012). More detailed information about the NCEP-CFSR reanalysis data set can be found in Saha *et al.* (2010).

In this study, surface wind fields (i.e., 10 m height) from three reanalyses, referred to as CFSR, MERRA, and ERA-Interim and an operational database referred to as ECMWF Operational, were obtained. The CFSR dataset covers the years 1979-2009 and has a temporal resolution of 1 hour and a spatial resolution of 0.312° x 0.312°. The MERRA dataset provides up-to-date data from the year 1979, with 1 hour of temporal and 1/2° x 2/3° spatial resolution. Both ECMWF data sets are available for the period between 1979 – present, and provide data with a temporal resolution of 6 hours and a spatial resolution of 0.250° x 0.250° (Table 1). These datasets do not have data at the measurement locations because they contain information at discrete grid points. Therefore, the closest four grid points of each data source (CFSR, MERRA, ERA-Interim, and ECMWF) to each measurement location were determined and the hindcast data at these grid points were extracted for the period of 2000 - 2014 for

Table 1. The specific features of every wind field dataset.

Data source	Institute	Temporal coverage	Temporal resolution	Spatial resolution
ERA-I	ECMWF	1979 - present	6-hourly	0.25° x 0.25°
OPER	ECMWF	1982 - present	6-hourly	0.25° x 0.25°
CFSR	NCEP	1979 - 2009	1-hourly	0.312° x 0.312°
MERRA	NASA	1979 - present	1-hourly	1/2° x 2/3°

the wind data sources. The coordinate information about the measuring locations and the grid points of each data source are given in Table 2. These points are shown in Figure 1 for all locations. The points marked as ECMWF in Fig. 1 represent the grid points of the ERA-Interim and ECMWF Operational data sources. These data sources have been abbreviated as ERA-I and OPER for ERA-Interim and ECMWF Operational, respectively, in the section presenting the analysis results.

Wind measurements

The measurements for the same period as the hindcast datasets were obtained from the TSMS for the five coastal locations along the southern Black Sea coast. These measurements are provided in universal time (UTC), with the hourly wind speed and direction at a reference height of 10 meters. The directions are adjusted in 12 sectors of 30° each, where North is centered at 0°. The requested data from the TSMS could not be completely obtained for all locations. The data collected from Gloria was measured at a height of 36 meters above the sea level at an interval of 6 hours and converted to the reference height of 10 m to enable a comparison with other data, as explained in the following Section 2.3.

Data collection and preparation

It is well known that large differences exist between wind measurements made onshore and those made offshore due to differences in surface roughness. Corrections, therefore, should be made to inland location data before they are applied to offshore regions. To facilitate such a correction, the power law wind distribution in the atmospheric planetary boundary layer (see, e.g., Davenport, 1965) is proposed. The power law has two significant characteristics that make it very useful for work involving the entire lower atmospheric boundary layer H; the law is a good average representation of the velocity profile over the entire atmospheric planetary boundary layer, and integral relationships based on this easily integrated law are close to being correct (see, e.g., Blackadar, 1960; Plate, 1971) (Hsu, 1980).

In an attempt to compare the performances of the wind fields, the measurement data at the coastal locations were converted to measurements on the sea. For the same reason, since the hindcast data were given at 10 m above sea level, all measurement data have also been brought to the same reference level. The wind measurements along the southern coast of the Black Sea are taken at coastal locations on land, so wind speed values at a 10 m height need to be converted into sea values by the following formula given by Hsu (1980):

$$U_{sea} = 3.0 * (\mathrm{U}_{land})^{2/3} \quad (1)$$

In the equation above, U_{land} and U_{sea} respectively represent the wind speeds measured at coastal locations and converted to open sea conditions. In deriving this equation, it was assumed that (1) the power law is valid both onshore and offshore and (2) the velocity on top of the atmospheric planetary boundary layer does not change appreciably across the coastal zone and that Z = 10 m. Essentially it assumes that there is a constant meso-wind speed that equal is over both land and sea, but different at sea levels due to different roughness factors. This transformation neglects the slow growth of offshore winds as one moves to more open areas (see, e.g., Taylor and Lee, 1984; Dobson *et al.*, 1989).

An elevation correction of the wind speed is needed because winds taken from observations often do not coincide with the standard 10-m reference level. The data recorded at the Gloria buoy location were available as wind measurements at 36 meters above the mean sea level. Therefore, these observations were converted to the 10-m reference level using two approximations for a proper comparison with hindcast data sets which are at a height of the 10-m reference level. For the case of winds taken in near-neutral conditions at a level near the 10-m level (within the elevation range of approximately 8-12 m), a simple approximation, the wind profile power law, is given as a 1/7 rule by US Army (2003) as:

$$U_{10} = U_z * (10 / z)^{1/7} \quad (2)$$

In this equation, z and U_z show the height where the measurements were recorded and the recorded wind speed, respectively. Another method to convert the wind measurements at 36 meters into wind speeds at 10 meters is using the log-law velocity V at a given height z (Onea and Rusu, 2012; Pimenta *et al.*, 2008):

$$V = V_{ref} \frac{\ln(z / z_0)}{\ln(z_{ref} / z_0)} \quad (3)$$

where z_{ref} and V_{ref} are respectively the height at which the measurements were recorded and the recorded wind speed values. The log-law assumes neutral atmospheric stability conditions under which the ground surface is neither heated nor cooled compared with the air temperature. The surface roughness length (z_0) is affected from the characteristics (such as the water surface; completely open terrain with a smooth surface, e.g., concrete runways in airports, mowed grass; larger cities with tall buildings; agricultural land with some houses and sheltering hedgerows 8 meters tall within a distance of approximately 500 meters, etc.) of the landscape. Different values for the surface roughness length are suggested for different landscape surfaces (Ragheb, 2017). The value of the calm sea surface roughness length (z_0) was taken as 0.2 mm based on Barthelmie *et al.* (1996) and Manwell *et al.* (2002), where the neutral stability of the atmosphere and a surface roughness were recommended as average values for calm and open seas, respectively (Pimenta *et al.*, 2008).

The data from the four nearest grid points were interpolated to each measurement location by applying two

Table 2. The coordinates of the locations of the measurements and the grid points of the wind fields, considered in this study.

Measurement Location	Grid Point	CFSR	MERRA	ECMWF	Measurement Location	Grid Point	CFSR	MERRA	ECMWF
Kumköy (41.25° N 29.04° E) 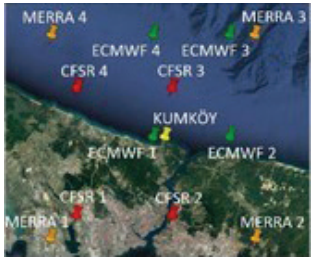	1	41.06° N 28.75° E	41.00° N 28.67° E	41.25° N 29.00° E	Giresun (40.92° N 38.39° E) 	1	40.75° N 38.13° E	40.50° N 38.00° E	40.75° N 38.25° E
	2	41.06° N 29.06° E	41.00° N 29.33° E	41.25° N 29.25° E		2	40.75° N 38.44° E	40.50° N 38.67° E	40.75° N 38.50° E
	3	41.37° N 29.06° E	41.50° N 29.33° E	41.50° N 29.25° E		3	41.06° N 38.44° E	41.00° N 38.67° E	41.00° N 38.50° E
	4	41.37° N 28.75° E	41.50° N 28.67° E	41.50° N 29.00° E		4	41.06° N 38.13° E	41.00° N 38.00° E	41.00° N 38.25° E
Amasra (41.75° N 32.38° E) 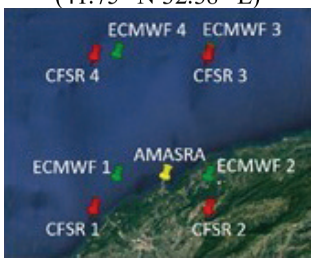	1	41.68° N 32.18° E	41.50° N 32.00° E	41.75° N 32.25° E	Hopa (41.41° N 41.43° E) 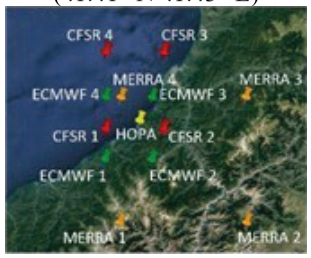	1	41.37° N 41.25° E	41.00° N 41.33° E	41.25° N 41.25° E
	2	41.68° N 32.50° E	41.50° N 32.67° E	41.75° N 32.50° E		2	41.37° N 41.56° E	41.00° N 42.00° E	41.25° N 41.50° E
	3	41.99° N 32.50° E	42.00° N 32.67° E	42.00° N 32.50° E		3	41.68° N 41.56° E	41.50° N 42.00° E	41.50° N 41.50° E
	4	41.99° N 32.19° E	42.00° N 32.00° E	42.00° N 32.25° E		4	41.68° N 41.25° E	41.50° N 41.33° E	41.50° N 41.25° E
Sinop (42.03° N 35.16° E) 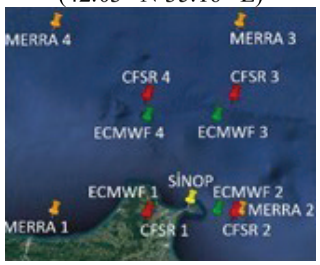	1	41.99° N 35.00° E	42.00° N 34.67° E	42.00° N 35.00° E	Gloria (44.52° N 29.57° E) 	1	44.49° N 29.38° E	44.50° N 29.33° E	44.50° N 29.50° E
	2	41.99° N 35.31° E	42.00° N 35.33° E	42.00° N 35.25° E		2	44.49° N 29.69° E	44.50° N 30.00° E	44.50° N 29.75° E
	3	42.31° N 35.31° E	42.50° N 35.33° E	42.25° N 35.25° E		3	44.81° N 29.69° E	45.00° N 30.00° E	44.75° N 29.75° E
	4	42.31° N 35.00° E	42.50° N 34.67° E	42.25° N 35.00° E		4	44.81° N 29.38° E	45.00° N 29.33° E	44.75° N 29.50° E

different methods. One of them is the inverse squared distance weighting interpolation function based on the values of the four nearest neighboring points. Denoting the wind speeds at the four grid points surrounding the buoy location as u_1, u_2, u_3 and u_4 and the corresponding distances from that location as r_1, r_2, r_3 and r_4, then the sought-for (model) wind speed, say U, is estimated by the expression:

$$U = \frac{\sum_{i=1}^{4}(u_i / r_i^2)}{\sum_{i=1}^{4}(1 / r_i^2)} \quad (4)$$

which gives the nearest points more influence (Soukissian and Papadopoulos, 2015). Another method is the area weighted average method (Macias J., personal communication). The area weighted average wind speeds, essentially bilinear interpolations in the wind speed, are calculated based on the following formula:

$$U = \frac{\sum_{i=1}^{4}(u_i * w_i)}{\sum_{i=1}^{4} w_i} \quad (5)$$

In this equation, represents the average wind speed, is the resultant wind speed computed from the wind speed components in the nearest grid points, and shows the areal weights, which are calculated according to the following equation:

$$w_i = (Dx - dx_i) * (Dy - dy_i) \quad (6)$$

Dx and *Dy* respectively represent the horizontal distances (zonal and meridional) between the grid points. The horizontal and vertical distances between the points and the buoy location were represented by dx_i and dy_i, respectively.

Probability distribution of the wind speeds

The probability distribution function graphs are obtained and the relationship between the hindcasted data and the measurements is examined. The Weibull function, which is one of the three most frequently used distributions (the others being Rayleigh and Lognormal) and seen by researchers as the most suitable distribution for wind data, is preferred (Celik, 2002). The 2-parameter Weibull probability density function was used here.

$$f(\mathrm{v}) = \left(\frac{k}{c}\right)\left(\frac{v}{c}\right)^{k-1} \exp\left[-\left(\frac{v}{c}\right)^{k}\right] \quad (7)$$

In this equation, v is the wind speed, k is the dimensionless shape parameter and c is the scale parameter.

The recommended method to use is the maximum likelihood method when determining these parameters for data sets in the form of a time series (Seguro and Lambert, 2000).

$$k = \left(\frac{\sum_{i=1}^{n} v_i^k \ln(v_i)}{\sum_{i=1}^{n} v_i^k} - \frac{\sum_{i=1}^{n} \ln(v_i)}{n} \right)^{-1} \quad (8)$$

$$c = \left(\frac{1}{n} \sum_{i=1}^{n} v_i^k \right)^{1/k} \quad (9)$$

In these equations, v is the wind speed, i is the time step, and n is the number of data points.

Results and Discussion

Statistical characteristics

The statistical parameters of the hindcasted and measured wind speeds were calculated and examined during 2004-2007 for each of the five coastal locations. Additionally, at the offshore buoy location (Gloria), the statistical parameters were also calculated using all available data in the years 2006-2009. They are presented in Table 3 for the coastal locations and Table 4 for the Gloria offshore location. The statistical parameters of the uncorrected and corrected measurements for the coastal locations are also presented. For the Gloria offshore location, in Table 4 the statistical characteristics are presented as converted to the measurements at 36 m and at 10 m based on the two approaches. Measurement 1 represents the obtained wind data based on Eq. 2 and Measurement 2 represents the obtained wind data based on Eq. 3.

The first noticeable thing in Table 3 is that the averages of the data obtained from the coastal measuring locations, which are not converted into winds over the sea, are significantly lower compared to all average values of the hindcast data sources. However, at the Gloria location the average of the measurements at 36 m is higher than that of the converted measurements to 10 m using both methods. The measurements converted into winds over the sea for the coastal locations and at a height of 10 m for the offshore location appear to have averages closer to the averages of the hindcast data sources than those of the uncorrected or unconverted measurements. Based on the corrected measurements at Kumköy in Table 3, it can be concluded that the average of the measurements appears to be generally very close to the averages of both ECMWF wind data sources, while the CFSR and MERRA winds have lower averages. The CFSR winds yielded rather close averages to that of the corrected measurements at Hopa, where the averages of the other winds were quite low. From Table 4 it can also be seen that the average value of the data denoted as Measurement 1 shows close results to that of the hindcast data sources and is nearest to that of the CFSR winds.

Table 3. The statistical parameters of the wind speeds between 2004 and 2007 for five coastal locations. The highlighted shows the nearest values to the corrected measurements. N refers to the number of data points.

Location	Data Source	N	Mean (m/s)	Median (m/s)	Max. (m/s)	Variance (m/s)	Standard deviation (m/s)	Coefficient of variation	Coefficient of skewness	Kurtosis
	Uncorrected measurements	31131	2.63	2.00	28.20	2.31	1.52	0.58	1.79	7.32
	Corrected measurements	31131	5.55	4.77	28.11	4.32	2.08	0.37	1.07	2.04
Kumköy	**CFSR**	35064	4.45	4.12	18.91	5.37	2.32	0.52	0.82	0.91
	MERRA	35064	4.60	4.36	15.48	4.83	2.20	0.48	0.68	0.54
	ERA-I	5844	5.65	5.29	20.95	8.42	2.90	0.51	0.76	0.73
	OPER	5844	5.63	5.31	18.11	7.88	2.81	0.50	0.74	0.66
	Uncorrected measurements	28560	4.39	3.60	25.20	9.01	3.00	0.68	1.11	1.10
	Corrected measurements	28560	7.68	7.08	26.07	12.81	3.58	0.47	0.65	-0.10
Amasra	**CFSR**	35064	4.59	4.29	20.74	5.05	2.25	0.49	0.77	0.84
	ERA-I	5844	5.22	4.90	19.53	6.69	2.59	0.50	0.65	0.40
	OPER	5844	5.00	4.55	18.15	7.85	2.80	0.56	0.77	0.36
	Uncorrected measurements	29994	2.88	2.50	44.20	3.89	1.97	0.68	1.69	9.07
	Corrected measurements	29994	5.81	5.54	37.98	7.02	2.65	0.46	0.86	1.38
Sinop	**CFSR**	35064	4.40	3.98	19.45	5.62	2.37	0.54	0.98	1.20
	MERRA	35064	3.93	3.77	12.39	3.39	1.84	0.47	0.53	0.15
	ERA-I	5844	4.71	4.44	16.77	5.67	2.38	0.51	0.66	0.43
	OPER	5844	5.31	4.95	18.27	8.00	2.83	0.53	0.68	0.26
	Uncorrected measurements	9515	1.85	1.50	41.10	2.70	1.64	0.89	12.99	240.54
	Corrected measurements	9515	4.38	3.94	36.17	3.38	1.84	0.42	6.46	83.38
Giresun	**CFSR**	35064	3.68	3.35	15.80	3.85	1.96	0.53	0.97	0.99
	ERA-I	5844	2.89	2.69	8.55	2.02	1.42	0.49	0.75	0.36
	OPER	5844	1.65	1.36	13.55	1.31	1.14	0.69	2.24	9.00
	Uncorrected measurements	13578	2.04	1.50	28.20	3.37	1.84	0.90	2.27	6.61
	Corrected measurements	13578	4.53	3.94	28.11	6.29	2.51	0.55	1.78	2.81
Hopa	**CFSR**	35064	3.87	3.44	14.65	4.92	2.22	0.57	0.98	0.99
	ERA-I	5844	2.33	2.19	7.80	1.24	1.12	0.48	0.53	-0.17
	OPER	5844	1.82	1.62	9.12	1.15	1.07	0.59	1.53	3.70

Table 4. The statistical parameters of the wind speeds for the Gloria location over the period of 2006-2009. The highlighted shows the nearest values to the corrected measurements. Measurement 1 represents the obtained wind data based on Eq. 2 and Measurement 2 represents the obtained wind data based on Eq. 3. N refers to the number of data points.

Data Source	N	Mean (m/s)	Median (m/s)	Max. (m/s)	Variance (m/s)	Standard deviation (m/s)	Coefficient of variation	Coefficient of skewness	Kurtosis
Measurement 1	5585	6.18	6.02	21.84	7.36	2.71	0.44	0.53	0.10
Measurement 2	5585	6.83	6.66	24.16	9.00	3.00	0.44	0.53	0.10
CFSR	35064	6.07	5.75	25.25	8.73	2.96	0.49	0.60	0.23
MERRA	35064	5.40	5.13	18.82	6.44	2.54	0.47	0.51	0.01
ERA-I	5844	5.50	5.21	18.83	7.18	2.68	0.49	0.55	0.08
OPER	5844	5.62	5.27	20.52	7.43	2.73	0.49	0.60	0.16

Regarding the maximum values, all the hindcast data sources have lower maximum values compared to those of the converted measurements at all measurement locations except for Sinop and Gloria, where the CFSR winds have maximum values higher than those of the measurements. At Amasra, Giresun, and Hopa, the maximum values of the wind speeds from the hindcast data sets are rather low in comparison with the measurements, while the CFSR winds are closer to those of the corrected measurements. At all coastal locations, the coefficient of variation, skewness, and kurtosis show that a decrease in the value occurred after converting the measurements to winds over the sea while there is no variation at the Gloria location for those of the converted measurements. The MERRA winds have closer coefficients of variation (COV) to that of the corrected measurements. At all measurement locations except Hopa, the COVs of the hindcast data sets are higher than those of the corrected or converted measurements. According to the skewness coefficient, all of the corrected measurements and hindcast data sets are right-skewed at all of the measurement locations. It appears that the CFSR winds have skewness values closer to those of the corrected measurements at Kumköy and Sinop, while at Hopa the skewness coefficients of the corrected measurements and the OPER winds are closer and the ERA-I dataset has a same value at Amasra. For the kurtosis coefficient, the last statistical parameter, kurtosis coefficients that are closer to the corrected measurements are observed in the OPER winds for Amasra and Hopa, the CFSR winds for Kumköy and Sinop, and the ERA-I winds for Gloria. Finally, it can be concluded that different wind data sources at different locations, and for different statistical indicators, have closer statistical values to those of the measurements.

Quality of the wind fields

This section describes the effect of applying different types of interpolation methods and assesses the effect of choosing land/sea effects on winds. The aim of this was to see the performance in the nearest grid point to the measurement location due to the proximity of the locations to the coast. The error statistics based on the data obtained using an area-weighted interpolation method at the measurement locations are given in Table 5. The error statistics based on the data from distance-weighted interpolation and each of the nearest four grid points surrounding the measurement locations for the wind data sources are also computed, but their results are not given here to save space. We see that some of the grid points considered in the interpolation may be far from the sea on the land side. In this case, due to the orographic effect, the poor performance in such a grid point will degrade the quality of the interpolated wind characteristic. Additionally, the results of the error statistics determined using both interpolation methods were very close to one another. Therefore, here we only present the results for the area-weighted interpolation method.

As for the error results (Table 5), it is seen that the ECMWF data sources show better performances in the majority of error parameters at Kumköy. The CFSR winds seem to have higher errors and lower correlations with a bias of 1.17 m/s, an HH index (Appendix B.6) of 0.44, and a correlation coefficient of approximately 0.58, followed the OPER winds with approximately 1.02 m/s, 0.40, and 0.65, respectively. At this location, the OPER winds have the best performance in terms of all error parameters. The error statistics based on four-year data at Amasra show much higher errors in terms of the bias, RMSE and MAE for all data sources (minimum bias = 2.52 m/s and a minimum RMSE = 3.88 m/s). The ERA-I winds have lower errors in terms of all error indicators compared to that of the CFSR and OPER winds. An HH value of 0.58 is obtained in the case of the ERA-I winds, followed by 0.62 for the OPER winds and 0.67 for the CFSR winds. At this location, the correlation coefficients are between 0.55 and 0.62. At Sinop, the OPER winds present the best performance, followed by the ERA-I, CFSR, and MERRA winds, respectively. The scatter indices vary from 46% and 51%, while the NMB (Appendix B.4) is between 9% and 33%. It is observed from the error analysis at Giresun that the CFSR winds have the best performance with a 0.54 m/s bias and an HH index, a 12% NMB, a 1.54 m/s MAE, and a 0.52 index of agreement (d). The second best performance is exhibited by the ERA-I winds, followed

Table 5. The statistical error values of the calculated wind speeds with area-weighted interpolation method from the data of the four nearest grid points to the measurement locations for the period of 2004-2007 at five coastal locations and the period of 2006-2009 at the Gloria offshore location.

Location	Data Source	N	bias (m/s)	NMB	RMSE (m/s)	HH	MAE (m/s)	d	SI	R
Kumköy	CFSR	31131	1.17	-0.21	2.30	0.44	1.86	0.71	0.41	0.58
	MERRA	31131	1.02	-0.18	2.13	0.40	1.68	0.73	0.38	0.61
	ERA-I	5368	0.00	0.00	2.20	0.37	1.74	0.78	0.39	0.65
	OPER	5368	-0.01	0.00	2.12	0.36	1.68	0.79	0.38	0.66
Amasra	CFSR	28560	3.15	-0.41	4.23	0.67	3.48	0.61	0.55	0.62
	ERA-I	4680	2.52	-0.33	3.88	0.58	3.18	0.65	0.51	0.58
	OPER	4680	2.67	-0.35	4.09	0.62	3.38	0.64	0.54	0.55
Sinop	CFSR	29994	1.40	-0.24	2.75	0.51	2.21	0.70	0.47	0.56
	MERRA	29994	1.91	-0.33	2.96	0.59	2.36	0.62	0.51	0.54
	ERA-I	5273	1.12	-0.19	2.72	0.49	2.15	0.69	0.47	0.52
	OPER	5273	0.50	-0.09	2.66	0.45	2.08	0.73	0.46	0.54
Giresun	CFSR	9515	0.54	-0.12	2.26	0.54	1.54	0.52	0.52	0.28
	ERA-I	2892	1.42	-0.32	2.20	0.58	1.79	0.51	0.49	0.33
	OPER	2892	2.77	-0.62	3.18	1.11	2.86	0.41	0.71	0.32
Hopa	CFSR	13578	0.67	-0.15	2.76	0.63	2.02	0.58	0.61	0.35
	ERA-I	4450	2.20	-0.48	3.17	0.91	2.34	0.49	0.69	0.44
	OPER	4450	2.69	-0.59	3.54	1.13	2.77	0.48	0.77	0.42
Gloria	CFSR	5585	-0.11	0.02	1.84	0.27	1.39	0.89	0.30	0.79
	MERRA	5585	0.74	-0.12	1.91	0.31	1.46	0.86	0.31	0.77
	ERA-I	5585	0.64	-0.10	1.75	0.28	1.34	0.89	0.28	0.81
	OPER	5585	0.52	-0.08	1.75	0.27	1.30	0.89	0.28	0.81

by the OPER winds with a poor performance with a scatter index of approximately 71% and a 62% NMB. At this location, the correlation coefficients between the hindcast and observation datasets are rather low. Our analysis is based on data from a few measurement locations, whereas the assimilation of the ERA data includes many measurement locations. It is therefore not that surprising that the assimilation process does not produce a good fit at all locations. The error statistics of the wind speeds at Hopa location are similar to the results at Giresun. It is understood that the CFSR winds with high spatial and temporal resolution show high performance in regions (south eastern part of the Black Sea) where the nearshore topographic structure is very variable. It should also be noted that the performances for wave hindcasts in the Hopa location in Van Vledder and Akpınar (2015) are better than the performances of the winds in the present study. The time series of the significant wave heights hindcasted from the default-setting SWAN model forcing with the reanalysis datasets used in the present study are very consistent with those of the measurements (please see Van Vledder and Akpınar, 2015 for additional information). However, we found in the present study that the wind measurements are rather low, especially in comparison with the wind speeds of the MERRA, ERA-I, and OPER at Hopa location. Cavaleri & Sclavo (2006) mentioned, especially for the generation of ECMWF datasets for coastal areas, that the model winds might not be reliable due to the important influence of orography that is not properly represented in the meteorological model because of its limited resolution (80 km for T255 of ERA-I). Staffell and Pfenninger (2016) also emphasized the spatial coarseness of the reanalyses relative to the microscale models for the low performances of the reanalyses. They stated that it is not possible to accurately represent the underlying atmospheric processes that generate wind speeds when the atmosphere is discretized into 50 × 50 km cells. Additionally, Azorin-Molina *et al.* (2018) mentioned that there may be a bias error for the wind measurements. Therefore, further research is required to develop methods to remove biases due to instrumental artifacts in observed wind speed series, such as improved calibration methods.

Table 5 also shows the statistical error analysis at the Gloria offshore drilling platform for the period of 2006 - 2009. The wind speeds converted according to Eq. (2) were used as observation data here. At this location the MERRA winds have the worst performance, probably due to its low spatial resolution. The lowest errors regarding the bias and NMB are observed as -0.11 m/s and 2% for the CFSR winds, respectively, but the best performances in terms of the RMSE (1.75 m/s), SI (28%), and correlation coefficient (0.81) are the OPER and ERA-I

winds at the Gloria location. It can be seen that at this offshore location values of correlation (approximately 0.8) are relatively high.

Based on all the above results, it can be concluded that the hindcast datasets against the measurements over the sea give lower error values compared to those against the measurements at the coastal locations due to various land-sea effects. There are essentially three characteristics (surface roughness, surface thermal and/or moisture properties, and surface elevation) of the terrain, whose spatial variation can cause variations in the near-surface wind field (see Hsu (1980); Taylor and Lee (1984) for more information). When examining the power law, it can be seen that the vertical variation of the wind along the profile is less affected over the low roughness surface than over the rough surface (see Hsu 1980). Therefore, the reanalysis wind fields are probably less affected over the sea and their performances are better at offshore areas than those at nearshore or coastal areas. The correlations between the hindcast data sets and the measurements at Hopa and Giresun are less than 50% and between 50% and 65% at the other coastal locations. The coefficients of the correlation were also higher (approximately 80%) at the Gloria offshore location in comparison with the coastal locations. This is an indication of the strong relationship between the measured and hindcasted wind speeds over open water, where wind fields are less influenced from high surface roughness variations on the land. This case shows that all wind fields can be used reliably at open sea areas in wave modeling but they may not be reliable at the coastal areas. Therefore, the high resolution regional wind hindcasts that are capable of solving the land-sea interaction for the coastal regions can be beneficial for accurate wave hindcasts.

Scatter diagrams of the hindcast data sets obtained using the area-weighted interpolation method against the measured wind speeds are given in Figures 2a and 2b for all measurement locations in order to give a clear illus-

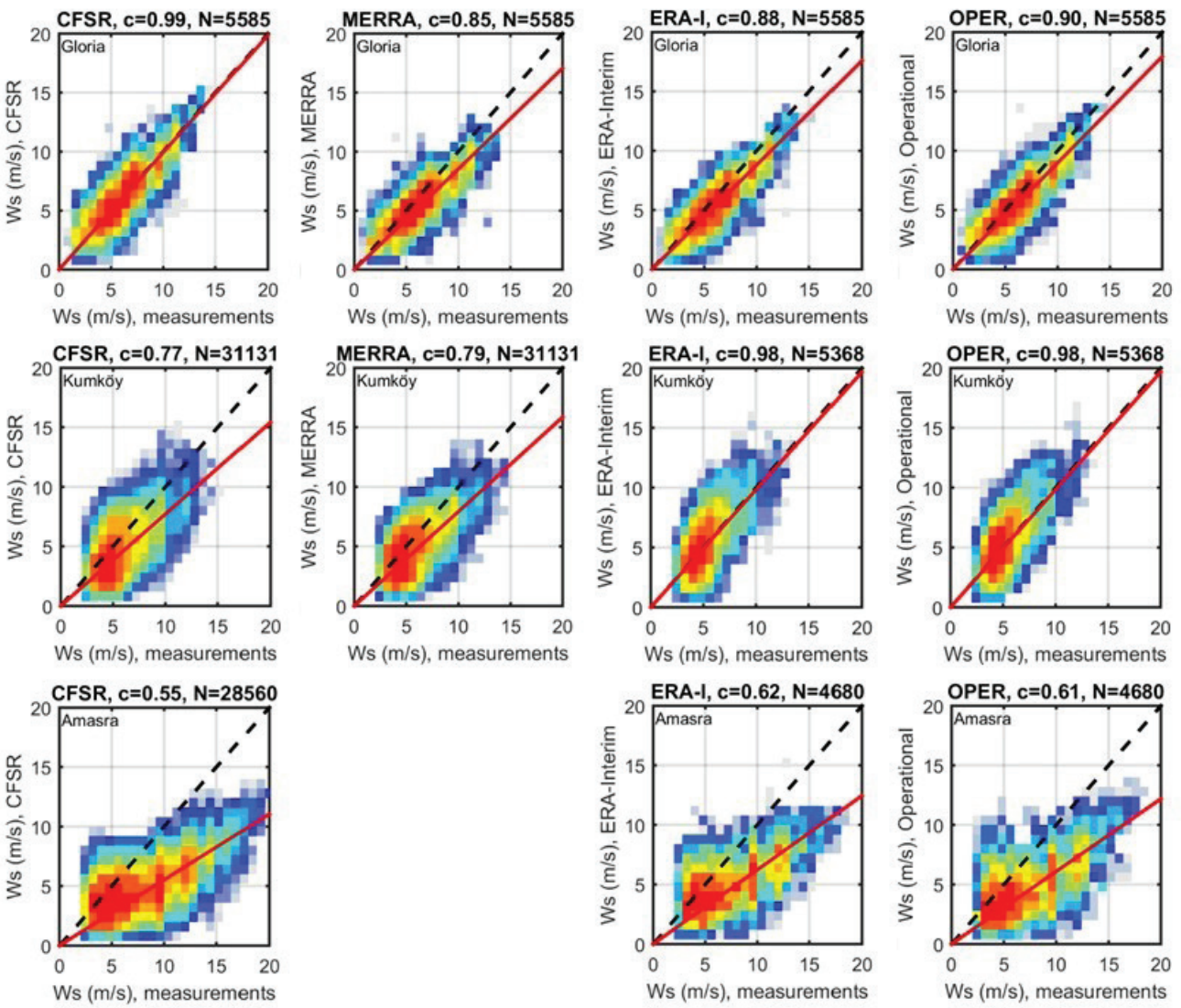

Fig. 2a: The scatter diagrams between the measurements and four different wind speeds calculated with the area weighted interpolation method from the four nearest grid points to the measurement locations for the data between 2006 and 2009 at the Gloria (upper panel), for the data between 2004 and 2007 at Kumköy (middle panel) and Amasra (bottom panel) locations. N refers the number of data points and $c = \sum(Y_i \; x \; X_i) / \sum(X_i)^2$

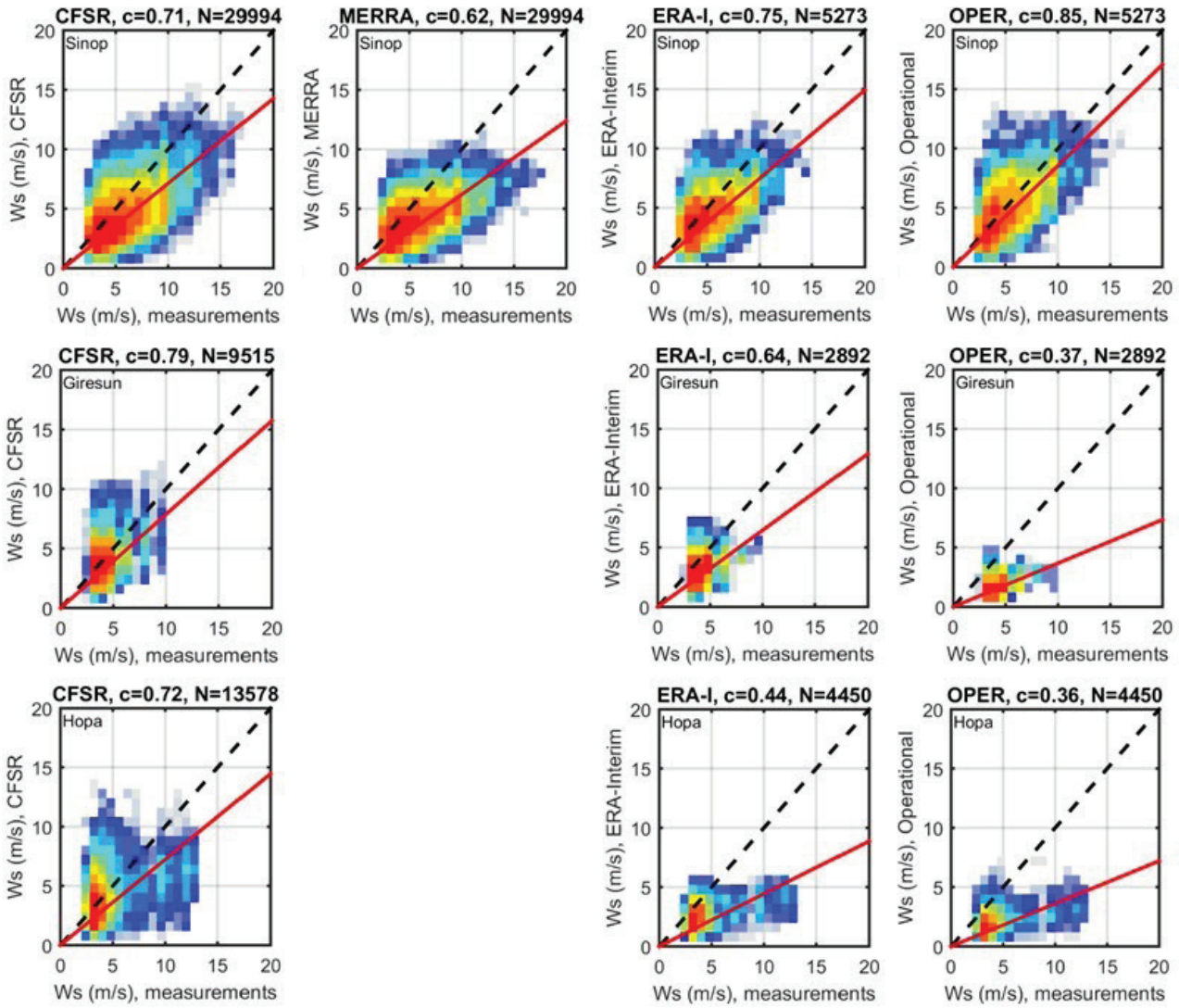

Fig. 2b: The scatter diagrams between the measurements and four different wind speeds calculated with the area weighted interpolation method from the four nearest grid points to the measurement locations for the data between 2004 and 2007 at Sinop (upper panel), Giresun (middle panel) and Hopa (bottom panel) locations. N refers the number of data points and $c = \sum(Y_i \; x \; X_i) / \sum(X_i)^2$

tration of the hindcast data sets' performances. The color scheme represents the log10 of the number of entries in a square box of 0.8 m/s, which is normalized with the log10 of the maximum number of entries in a box. In this way, the clustering of the data points is highlighted. Each figure contains 2 lines. The red line represents the model y=cx and the line of perfect agreement is the dashed line. The number of samples N, correlation coefficients, and the names of the winds are shown in the title. These figures show that the trend line of the CFSR winds overlaps with that of the measurements, although the trend lines of all the datasets are close to the 45 degree line, showing the almost perfect relationship at the Gloria location. Furthermore, it is observed that the hindcast data sets are more coherent with the measurements at Gloria in comparison with the coastal locations.

In addition to the bulk data error analysis, the analysis of the extremes is of utmost importance. For this purpose, here the annual and seasonal maximum values of both measurements and each wind data source, as well as the 95th and 99th percentile wind speeds are determined and compared. The results for the period of 2004-2007 at the coastal locations and 2006-2009 at Gloria are presented in Tables 6 and 7. While the CFSR winds give closer results to the corrected wind speeds in terms of 95th and 99th percentile wind speeds at Kumköy, the different wind data sources at different years show results closer to the corrected measurements for annual extremes. At other coastal locations, except Hopa where the CFSR winds perform well, almost all of measured extremes are estimated low by the wind fields. At Gloria, the wind extremes from Measurement_2 are represented rather well by the CFSR winds. The statistics of the extremes in Table 6 also shows that higher-speed winds are often seen along the southwestern coast of the Black Sea in comparison with the ones in the east.

In addition to the comparison of the statistics of annual and seasonal extremes, we also focused on peak events

Table 6. The 95th and 99th percentiles, annual and seasonal maxima of the wind speeds for years between 2004-2007 for the coastal locations. The highlighted shows the nearest values to the corrected measurements.

Location		95th-prc Wind Speed (m/s)	99th-prc Wind Speed (m/s)	Annual Maximum Wind Speeds (m/s)				Seasonal Maximum Wind Speeds (m/s)			
				2004	2005	2006	2007	Winter	Spring	Summer	Autumn
Kumköy	Uncorrected Measurements	5.60	7.70	11.30	14.40	28.20	13.80	14.40	28.20	7.70	11.30
	Corrected Measurements	9.51	11.78	15.23	17.92	28.11	17.41	17.92	28.11	11.78	15.23
	CFSR	8.62	11.09	18.91	13.99	15.92	13.83	18.91	12.24	12.43	13.54
	MERRA	8.57	10.71	15.48	12.06	14.23	11.53	15.48	11.67	10.58	11.98
	ERA-I	10.95	13.68	20.95	16.39	19.00	14.05	20.95	15.04	14.59	17.95
	OPER	10.94	13.46	18.11	16.60	17.87	15.19	18.11	14.24	14.57	17.24
Amasra	Uncorrected Measurements	10.20	13.30	19.00	18.50	19.50	25.20	19.50	25.20	19.50	20.00
	Corrected Measurements	14.22	16.99	21.57	21.19	21.95	26.07	21.95	26.07	21.95	22.33
	CFSR	8.69	10.96	14.23	13.92	14.16	20.74	17.33	14.12	13.51	20.74
	ERA-I	9.88	12.22	14.96	14.15	15.35	19.53	15.95	14.15	15.15	19.53
	OPER	10.26	12.86	15.65	14.68	17.29	18.15	17.29	14.68	15.48	18.15
Sinop	Uncorrected Measurements	6.60	9.70	14.40	16.40	13.80	44.20	44.20	16.40	11.30	14.90
	Corrected Measurements	10.62	13.75	17.92	19.55	17.41	37.98	37.98	19.55	15.23	18.33
	CFSR	9.06	11.40	19.31	14.21	16.84	19.45	19.45	15.25	14.21	14.77
	MERRA	7.24	8.78	11.70	10.95	11.87	12.39	11.87	11.68	8.59	12.39
	ERA-I	9.12	11.23	14.49	13.46	15.50	16.77	14.07	15.50	11.29	16.77
	OPER	10.57	13.01	17.12	15.87	18.27	17.88	17.12	18.27	14.59	17.88
Giresun	Uncorrected Measurements	4.10	5.10	20.50	41.10	33.40	9.20	36.00	41.10	30.80	38.50
	Corrected Measurements	7.72	8.94	22.70	36.17	31.48	13.27	33.10	36.17	29.82	34.62
	CFSR	7.56	9.54	11.54	13.84	11.10	15.80	15.80	11.77	9.16	12.48
	ERA-I	5.56	6.99	8.32	7.79	8.37	8.55	8.32	8.37	5.98	8.55
	OPER	3.75	5.83	5.40	4.87	7.54	13.55	10.96	9.55	5.06	13.55
Hopa	Uncorrected Measurements	6.60	8.20	9.20	13.30	10.20	28.20	28.20	13.30	9.20	10.20
	Corrected Measurements	10.62	12.29	13.27	16.99	14.22	28.11	28.11	16.99	13.27	14.22
	CFSR	8.11	10.40	14.65	14.10	14.24	14.06	14.61	13.78	9.50	14.65
	ERA-I	4.36	5.20	5.63	7.16	6.28	7.80	6.28	7.16	5.40	7.80
	OPER	3.89	5.57	4.82	4.57	8.12	9.12	7.95	7.66	6.09	9.12

Table 7. The 95th and 99th percentiles, annual and seasonal maxima of the wind speeds for years between 2006 and 2009 for the Gloria location.

	95th-prc Wind Speed (m/s)	99th-prc Wind Speed (m/s)	Annual Maximum Wind Speeds (m/s)				Seasonal Maximum Wind Speeds (m/s)			
			2006	2007	2008	2009	Winter	Spring	Summer	Autumn
Measurement_1	10.54	12.80	15.81	21.84	17.32	14.31	17.32	15.06	12.80	21.84
Measurement_2	11.66	14.16	17.49	24.16	19.16	15.83	19.16	16.66	14.16	24.16
CFSR	11.49	14.08	17.50	25.25	17.50	15.42	19.00	17.52	15.42	25.25
MERRA	10.10	12.05	13.79	18.82	15.42	13.41	15.03	14.20	12.35	18.82
ERA-I	10.41	12.71	14.74	18.83	15.67	14.40	15.67	15.69	12.44	18.83
OPER	10.68	12.94	14.19	20.52	15.99	15.77	15.99	15.89	12.77	20.52

based on an analysis of the observed wind speed peaks and associated hindcasted peaks. For the peak selection, a threshold level was defined at the 90% quantile of all wind speeds as observed at each location. Next, the highest peaks in each time interval in which the observed wind speed exceeds this threshold were taken. For the statistical analysis, the selected observed peaks were colocated with the nearest highest peak within a time interval of 48 h on each side to allow for some phase shift in reaching the peak levels. The results of this statistical analysis are shown in Fig. 3. The threshold levels for each location are given in the figure title. The results indicate that the ECMWF winds at Kumköy and Amasra and CFSR winds at Hopa and Gloria perform better than the others. For all wind fields the wind speed peaks are significantly underestimated at all the coastal locations, but at Gloria they perform well. These results are consistent with our previous findings.

Wind roses

In this section, the compatibility of the measurement data and the wind fields has been analyzed in terms of the wind directions and speed distributions. Wind roses for all locations were created using four-year data for each location. The directions are separated in 12 sectors of 30° each, where north is centered at 0°. The wind roses of the measurements and hindcast data of the grid points are presented in Figs. 4a-4c. The wind speeds for Number 3 are those for the Kumköy location, Number 4 for all winds at Hopa, Number 1 for the ECMWF winds and Number 2 for the CFSR and MERRA winds at Gloria. In terms of wind frequency, the dominant winds appear to blow from the east at Kumköy, as shown in Figure 4a. Storms, however, seem to originate from the Northern and Southern directions. A 12.5-degree deviation is witnessed in the estimation of northeastern winds, while southeastern winds are not captured in the wind roses of the wind fields. Strong winds from the northern direction are captured in the wind roses representing hindcasts. However, this fails to capture storms originating from the southern direction. At this location, all wind fields present a similar directional distribution to one another, showing a strong channeled flow where dominant directions are observed as north-easterly. The spatial distributions of all wind fields around this location are plotted in Figure 5a for November 28, 2007, 12:00 pm to see whether orographic effects are a channeled or tunneling flow on the wind fields. This figure shows that wind field products are not affected as directionally around this location. The wind speeds decrease on land in comparison with the sea but their directions are not affected by this case, although there is an average land height of approximately 100 m. It can finally be concluded that missing orographic effects around the Kumköy location affect the accuracy of the wind fields.

Wind roses of the measurements at Amasra (not shown here) show that the directions of the prevailing and secondary winds are south-southeast (SSE) and east-northeast (ENE), while most storms observed blow mainly from four direction sectors west (W), SSE, ENE, and northeast (NE). It is interesting that the secondary direction at the measurements is observed as the prevailing direction at all hindcast winds. At Sinop (not shown here), the prevailing winds blow from the northwest (NW) and both dominant and secondary directions are estimated with 12.5 degrees of deviation at all hindcast winds. The wind roses of the measurements at Giresun (not shown here) and Hopa (Fig. 4b) have no similarities to the wind roses for the hindcast data sources. The directional distributions of the CFSR and OPER winds are very similar at both these locations. At the Gloria location, the wind roses of all hindcast data sets show a similar behavior to those of the measurements (Fig. 4c). Figs. 5b and 5c show spatial distributions of the wind fields for November 28, 2007 12:00 pm around Hopa and Gloria. The mountains in the eastern Black Sea region (and around Hopa) rise rapidly from the coast and are parallel to the shore. They reach a height of 3500 m after approximately 35-40 km from the sea. Consequently, it is expected that they will affect the winds fields, as seen in Figure 5b. This figure shows that, at Hopa, all wind fields are affected from the orographic effects in terms of both directionally and

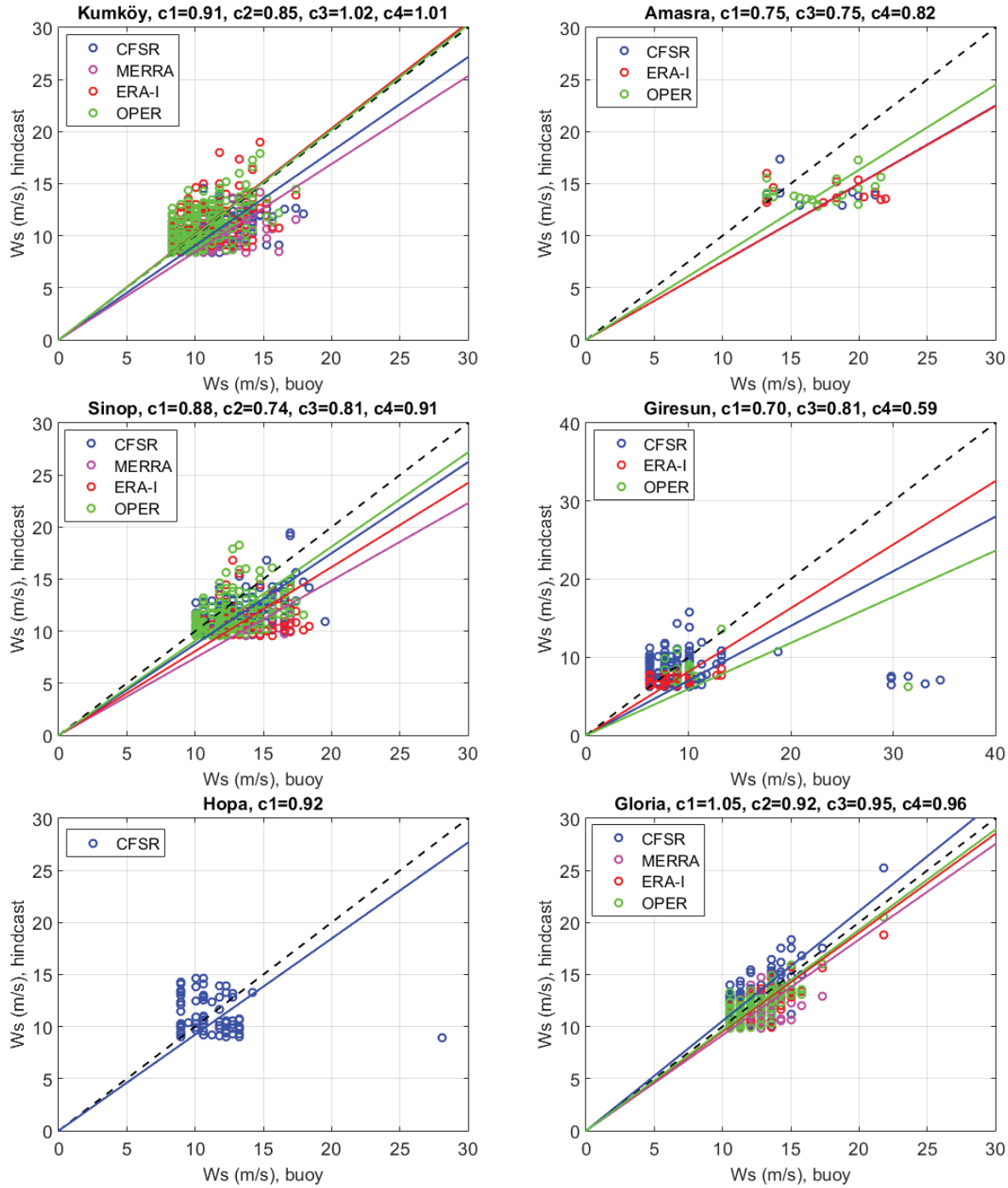

Fig. 3: The comparison of the observed and hindcasted peaks of the wind speeds at the measurement locations using the 90% quantile of all observed wind speeds per location. $c = \sum(Y_i \, x \, X_i) / \sum(X_i)^2$ and the coefficients from c_1 to c_4 are for the CFSR, MERRA, ERA-I, and OPER winds, respectively. Threshold values are 8.34 m/s for Kumköy, 12.78 m/s for Amasra, 9.52 m/s for Sinop, 6.26 m/s for Giresun, 8.94 m/s for Hopa, and 9.79 m/s for Gloria.

severity of winds. The intensity of the winds decreases and they change direction. However, although the wind fields perceive an effect of a high mountainous regions, they have insufficient spatial resolution to be accurately included this orographic effect. Howard and Clark (2007) suggest a method for reconciling the observed and modeled wind speeds for unresolved orography parameterization based on the linear theory of a neutral boundary-layer flow over hills and included a resolution of both problems, one of which is the artificially increased surface stress that caused a reduction in the predicted wind speed at the standard wind observing height of 10 m, and the other is the speed-up over the unresolved summits, which are not modeled.

For the Gloria location, it is seen from Fig. 5c that, because the measuring location is far from the coast and in the open sea, the wind fields are not affected from orographic effects and they are consistent with the measurements.

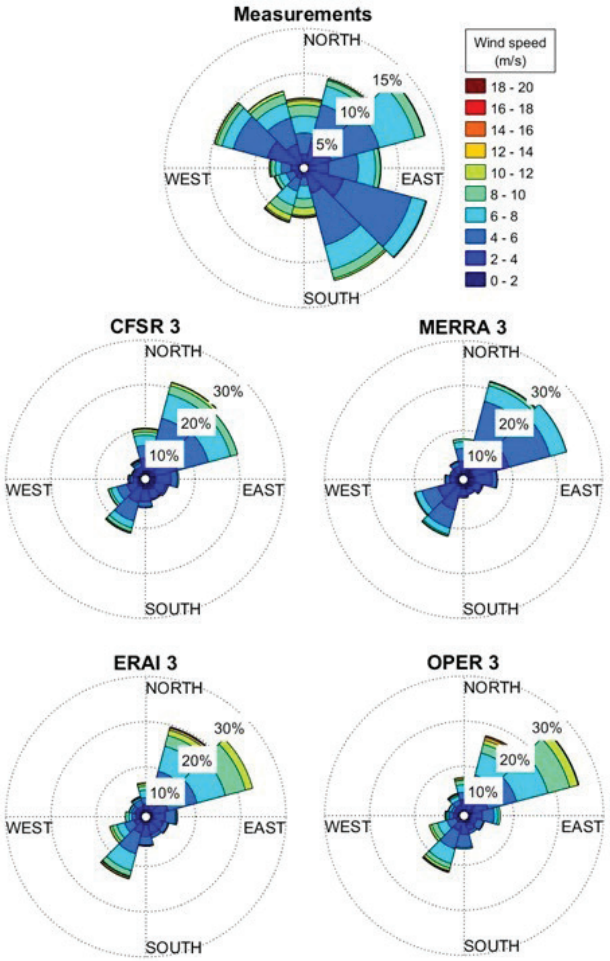

Fig. 4a: The wind roses of the measurements and wind fields at Kumköy in years between 2004 and 2007. Title shows both wind forcings and the number of the grid point.

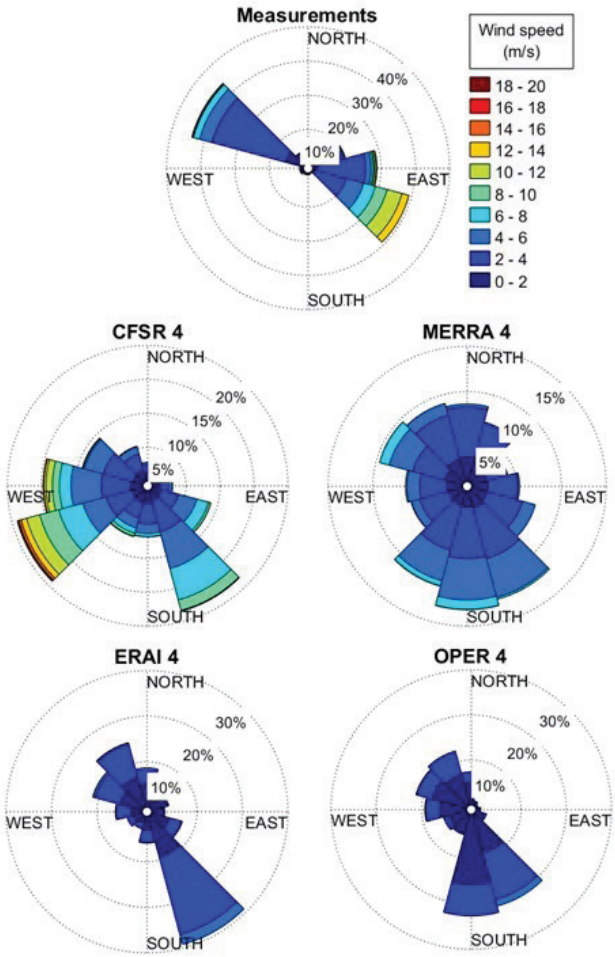

Fig. 4b: The wind roses of the measurements and wind fields at Hopa in years between 2004 and 2007. Title shows both wind forcings and the number of the grid points.

Probability distributions

The performances of wind data sources were evaluated by comparing the Weibull probability distributions for all four types of hindcasted, wind fields and measured wind speeds at the five coastal locations and the one offshore location. First, the probability distributions of all types of hindcast data were determined in all sets of the four grid points surrounding each measurement location and those based on the two interpolation methods. Hereafter, these data were intercompared as shown in Figure 6, in which only the area-weighted interpolation method was selected for presentation. The graph representing the Kumköy location shows that the distributions of the CFSR and MERRA data sources appear to be shifted to lower wind speed values, although they have a similar shape. This indicates that for these wind data sources, weak winds have a high frequency, while strong winds have a low frequency of occurrence in this location. Additionally, it is observed that the peak wind speeds are underestimated by these data sources. The peak values of the wind speeds estimated with the two different ECMWF's data sources (ERA-I and OPER) are better in comparison with the CFSR and MERRA winds. There are, however, also some differences, for example, the probability distributions of the wind speeds from the ECMWF data sets are more flattened than that of the measurements. At Amasra, the wind speeds of all wind fields exhibited very different distributions in comparison with those of the measurements. This also occurred for the MERRA winds at Sinop where the CFSR and ERA-I winds have similar distributions to those of the measurements. The probability distributions of the OPER winds and the measurements are very similar at this location. Although, at Giresun the CFSR and ERA-I winds have similar distributions to those of the measurements; the CFSR winds have a lower probability while the ERA-I winds have a higher probability at low values. There is also an interesting case, which is the considerably large difference between the distributions of data from the OPER wind fields and measurements. The ECMWF data sources have much broader distributions that cannot represent the measurements at Hopa. The closest distribution to those of the measurements is seen in the CFSR wind fields at this location. At Gloria, the distribution of the converted measurements using the log-law (Eq. 3) are more dispersed than those of the measurements converted using the power law (Eq. 2). It is assumed that these differences are because the log-law approach is highly dependent on the correctness of the roughness and the convective boundary layer phe-

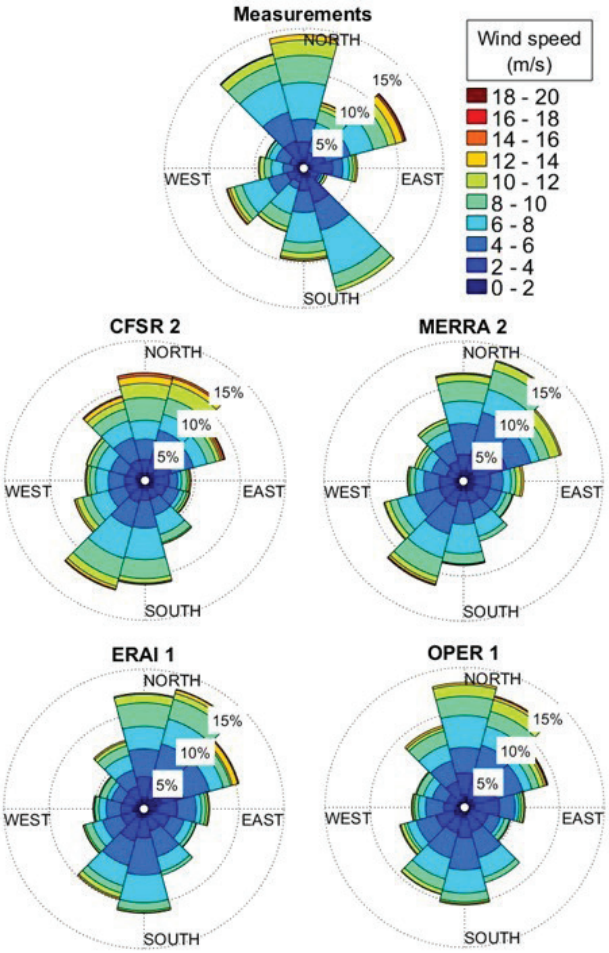

Fig. 4c: The wind roses of the measurements and wind fields at Gloria in years between 2006 and 2009. Title shows both wind forcings and the number of the grid point.

nomena, whereas the power-law to the wind shear, which is highly variable during the day, has a seasonal shifting and is influenced heavily by atmospheric stability assumptions. Here, data from the CFSR wind fields seem to be closer to the measurements corrected using both equations. The measurements data calculated using Eq. 2 have distributions similar to the ERA-I and OPER winds. The CFSR winds have a flatter peak while the MERRA winds have a sharper peak. The data distributions resulting from the application of Eq. 3 had a fair agreement with the CFSR winds as opposed to the other winds that had rather sharper peak. The wind speed outputs, which better overlap to the probability distributions of the measurements, imply a reduction of the uncertainties in the wind-wave modeling estimates. Overlapping the measured and hindcasted probability distributions, especially in moderate and extreme wind conditions, can provide more accurate wave estimates for moderate and extreme wave conditions, which are very important in the design of coastal structures. A general conclusion is that there is no kind of wind input that performs best at all locations.

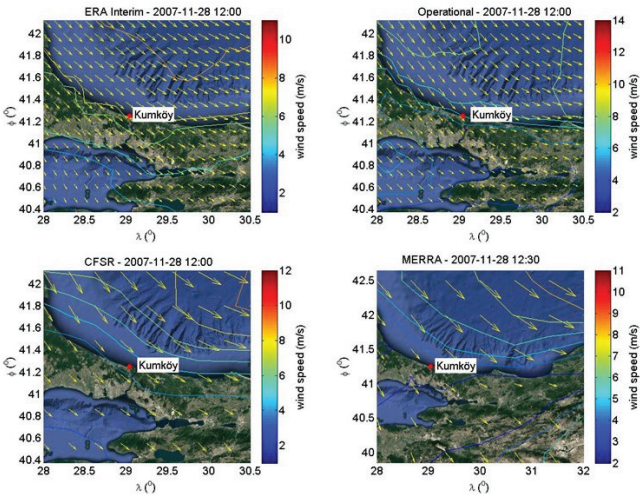

Fig. 5a: The spatial distribution of the wind speed and wind direction at wind model nodes around Kumköy for 28 November 2007 12:00 pm. The arrows are scaled with the wind speed magnitude.

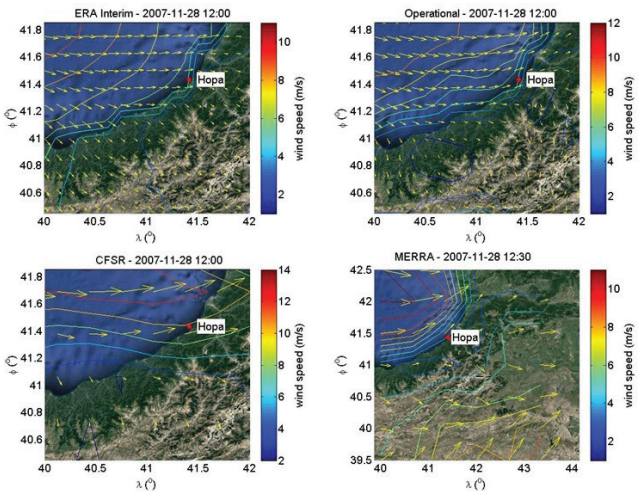

Fig. 5b: The spatial distribution of the wind speed and wind direction at wind model nodes around Hopa for 28 November 2007 12:00 pm. The arrows are scaled with the wind speed magnitude.

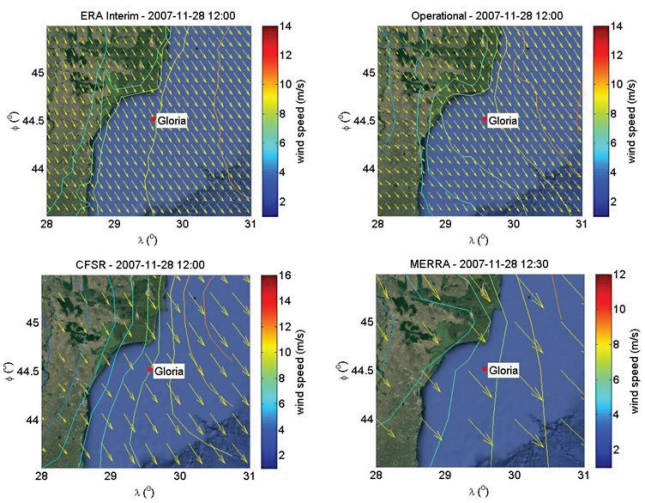

Fig. 5c: The spatial distribution of the wind speed and wind direction at wind model nodes around Gloria for 28 November 2007 12:00 pm. The arrows are scaled with the wind speed magnitude.

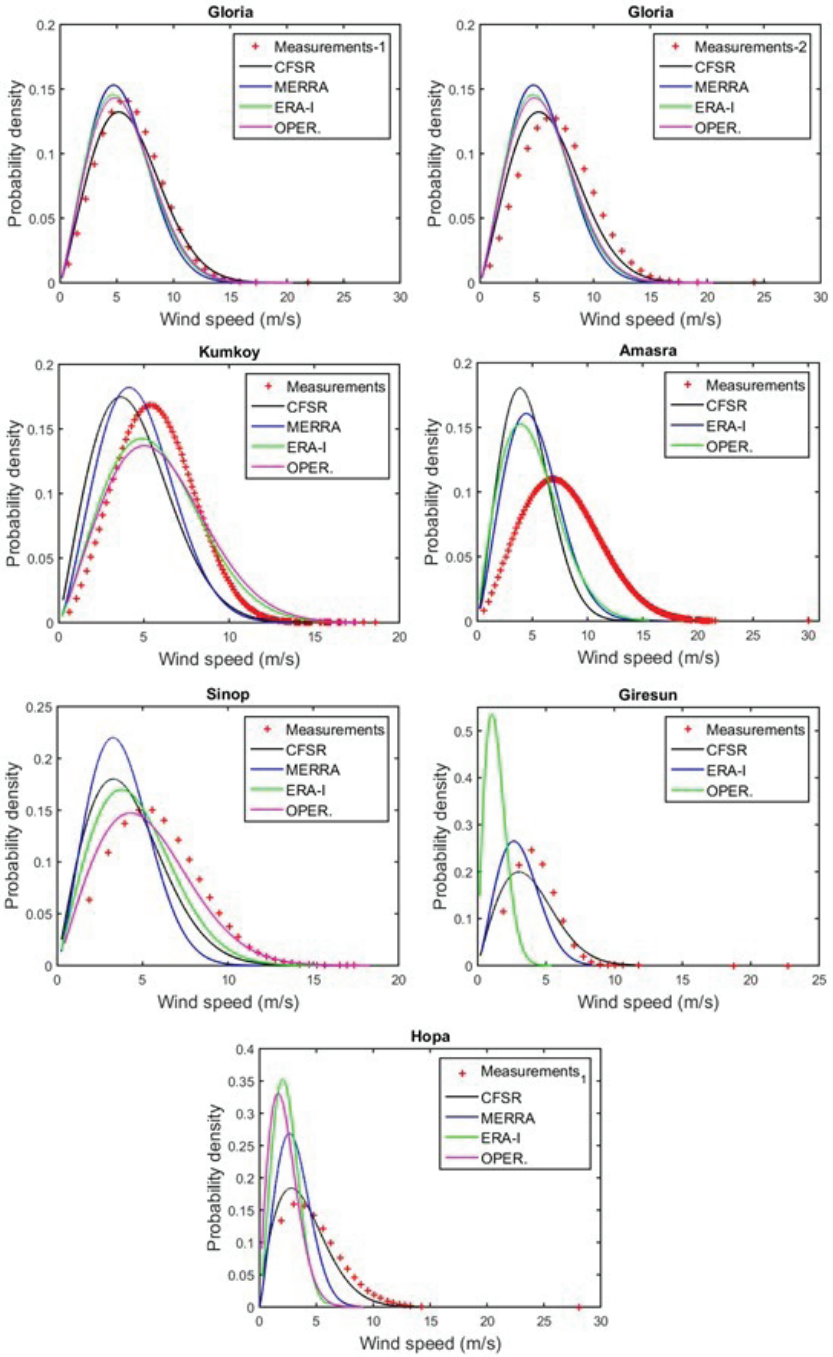

Fig. 6: The comparison of the probability distributions of the wind speeds, calculated by the area-weighted interpolation method, against the measurements at the Gloria (for Measurement-1 and 2), Kumköy, Amasra, Sinop, Giresun and Hopa.

Quality of the wind fields for different wind speed intervals

The quality of moderate and extreme winds is very important in wind power development and wave modeling because it determines or affects the amount of wind energy that is to be captured by wind power plants and the accurate hindcasting of extreme waves, which is the main determinant factor in the design of coastal structures. Therefore, the measured wind speeds were classified into regular intervals, and then the performances of the wind fields at these speed ranges were examined based on the error analysis results to determine their qualities at different wind speed intervals. The results from the statistical error analysis between the observed and hindcasted wind speeds in different wind speed ranges for the period of 2004-2007 at the coastal locations and 2006-2009 at the Gloria offshore location are presented in Tables 8-11. The error statistics for the low-speed winds (0 m/s <WS<4 m/s) are given in Table 8. The correlations between the hindcasted and measured wind speeds are rather low (< 0.50) for low-speed winds at all locations. At Kumköy, the MERRA winds performed very well at low speeds with a 1.49 m/s RMSE and a 43% SI, and the CFSR winds came in second with a 1.61 m/s RMSE and a 46% SI. At Amasra, the CFSR winds are on top with a bias of

Table 8. The statistical error values of all wind fields for the wind speed range between 0 m/s - 4 m/s for 2004-2007 for the coastal locations and 2006-2009 for the Gloria offshore location.

Location	Data Source	N	bias (m/s)	NMB	RMSE (m/s)	HH	MAE (m/s)	d	SI	r
Kumköy	CFSR	9493	0.26	-0.07	1.61	0.48	1.31	0.40	0.46	0.17
	MERRA	9493	0.10	-0.03	1.49	0.43	1.20	0.41	0.43	0.14
	ERA-I	1631	-0.41	0.12	1.84	0.50	1.45	0.37	0.53	0.17
	OPER	1631	-0.41	0.12	1.81	0.49	1.41	0.38	0.52	0.19
Amasra	CFSR	5440	0.06	-0.02	1.65	0.50	1.32	0.38	0.49	0.06
	ERA-I	935	-0.53	0.16	2.12	0.59	1.62	0.32	0.64	0.05
	OPER	935	-0.34	0.10	2.38	0.68	1.82	0.29	0.72	0.02
Sinop	CFSR	10173	-0.07	0.02	1.75	0.54	1.37	0.41	0.56	0.18
	MERRA	10173	0.22	-0.07	1.54	0.50	1.24	0.45	0.49	0.18
	ERA-I	1821	-0.30	0.09	1.98	0.59	1.53	0.37	0.62	0.16
	OPER	1821	-0.64	0.20	2.29	0.65	1.73	0.35	0.72	0.20
Giresun	CFSR	5684	0.01	0.00	1.63	0.47	1.24	0.32	0.47	0.05
	ERA-I	1584	0.72	-0.21	1.56	0.51	1.30	0.34	0.45	0.04
	OPER	1584	1.99	-0.58	2.30	1.03	2.11	0.27	0.67	-0.08
Hopa	CFSR	9317	-0.17	0.05	1.89	0.57	1.42	0.32	0.59	0.13
	ERA-I	3035	1.12	-0.35	1.56	0.60	1.32	0.35	0.48	0.10
	OPER	3035	1.61	-0.50	1.91	0.84	1.72	0.31	0.59	0.08
Gloria	CFSR	1326	-0.74	0.25	1.80	0.55	1.37	0.44	0.62	0.24
	MERRA	1327	-0.23	0.08	1.49	0.48	1.11	0.52	0.51	0.28
	ERA-I	1326	-0.16	0.06	1.39	0.46	1.08	0.57	0.48	0.35
	OPER	1326	-0.28	0.10	1.39	0.45	1.06	0.55	0.48	0.33

0.06 m/s and a 49% SI at low wind speeds. The Sinop location has the MERRA winds as the best followed by the CFSR winds at low speeds. At Giresun, the CFSR winds present the best results at low speeds. At the Hopa location, the MERRA winds have the best results at low wind speeds followed by the ERA-Interim winds. It was observed in Table 8 that ERA-I winds are better at low speeds, displaying a 6% NMB, a 1.39 m/s RMSE and a 48% SI at the Gloria location, while the CFSR winds are inferior at this location have an RMSE and SI of 1.80 m/s and 62%, respectively.

The statistical error values of all wind fields for moderate wind speed ranges (4 m/s – 8 m/s and 8 m/s – 12 m/s) for 2004 – 2007 for the coastal locations and 2006 – 2009 for the Gloria offshore location are presented in Tables 9 and 10. At Kumköy, the best performance at moderate wind speeds was obtained from the ECMWF winds. The values of 2.49 m/s for the RMSE and 26% for the SI at a high wind speed range (8 m/s-12 m/s) make the OPER the best. At Amasra, ERA-I winds performed better based on all error parameters at moderate wind speeds. At the Sinop location, at moderate wind speeds the OPER winds had a 3.08 m/s RMSE and a 33% SI, making them the best performer. The CFSR winds presented the best results, displaying the lowest error values at moderate wind speeds at Giresun and Hopa. In the case of the moderate wind speed range, at Gloria the CFSR winds were the best performer, producing a 1.83 m/s RMSE and a 19% SI in the range of 8 m/s-12 m/s.

Table 11 gives statistical error values of all wind fields for a wind speed range greater than 12 m/s for 2004-2007 for the coastal locations and 2006-2009 for the Gloria offshore location. At Kumköy, it is seen that ECMWF winds performed excellently by having a 4.05 m/s RMSE and a 31% SI. The ECMWF winds were also better against the CFSR winds for severe winds (>12 m/s) at Amasra. At Sinop, it was found that the CFSR winds came in first in performance in this speed range with a 5.29 m/s RMSE and a 39% SI. At Giresun, for the ECMWF winds it appeared that there was almost no temporal matching of data (n = 4) for values above the 12 m/s wind speeds. Although there were a few matching data (n = 26) between the measurements and the CFSR winds for speeds over 12 m/s, this was still not sufficient for an assessment of the error statistics. However, the CFSR winds can be accepted as the best, considering the amount of data and error statistics at this location. At the Hopa location, at severe wind speeds CFSR winds displayed the lowest error values. For severe wind speeds, the CFSR winds had the best accuracy with a 2.18 m/s RMSE and a 17% SI at the Gloria offshore location.

Tables 8-11 show that, at Gloria, the errors of all wind fields decrease with an increasing wind speeds. The CFSR winds have higher errors at low winds but lower errors at severe winds in comparison with others at this location. The MERRA winds present a better performance at low

Table 9. The statistical error values of all wind fields for the wind speed range between 4 m/s - 8 m/s for 2004-2007 for the coastal locations and 2006-2009 for the Gloria offshore location.

Location	Data Source	N	bias (m/s)	NMB	RMSE (m/s)	HH	MAE (m/s)	d	SI	r
Kumköy	CFSR	17854	1.38	-0.24	2.35	0.46	1.96	0.46	0.41	0.34
	MERRA	17854	1.24	-0.21	2.16	0.42	1.76	0.48	0.37	0.38
	ERA-I	3046	0.16	-0.03	2.24	0.39	1.80	0.51	0.39	0.40
	OPER	3046	0.12	-0.02	2.14	0.37	1.74	0.53	0.37	0.42
Amasra	CFSR	11286	2.24	-0.37	2.87	0.59	2.46	0.37	0.47	0.17
	ERA-I	1840	1.85	-0.30	2.79	0.55	2.37	0.38	0.46	0.15
	OPER	1840	2.01	-0.33	3.05	0.61	2.61	0.36	0.50	0.13
Sinop	CFSR	14113	1.64	-0.27	2.62	0.50	2.23	0.42	0.43	0.23
	MERRA	14113	2.06	-0.34	2.66	0.54	2.29	0.40	0.44	0.24
	ERA-I	2437	1.28	-0.21	2.48	0.46	2.05	0.42	0.41	0.20
	OPER	2437	0.66	-0.11	2.53	0.44	2.06	0.43	0.42	0.21
Giresun	CFSR	3611	1.09	-0.20	2.13	0.43	1.76	0.46	0.39	0.31
	ERA-I	1245	2.14	-0.39	2.61	0.60	2.26	0.39	0.47	0.24
	OPER	1245	3.59	-0.65	3.82	1.15	3.64	0.31	0.69	0.26
Hopa	CFSR	2710	1.06	-0.19	2.79	0.54	2.31	0.35	0.49	0.08
	ERA-I	899	3.09	-0.54	3.38	0.86	3.10	0.34	0.59	0.17
	OPER	899	3.52	-0.61	3.82	1.07	3.56	0.32	0.67	0.12
Gloria	CFSR	2929	-0.02	0.00	1.84	0.31	1.39	0.58	0.31	0.44
	MERRA	2928	0.70	-0.12	1.78	0.32	1.38	0.58	0.30	0.43
	ERA-I	2929	0.67	-0.11	1.71	0.30	1.33	0.60	0.29	0.46
	OPER	2929	0.57	-0.10	1.69	0.30	1.29	0.61	0.29	0.47

winds at the south western locations of Kumköy, Amasra, and Sinop of the Black Sea. The ECMWF and OPER winds have lower errors at moderate and severe winds at these locations, respectively. At the Giresun and Hopa locations in the south eastern part of the Black Sea, the ERA-I winds show lower errors at low winds while the CFSR winds have lower errors at moderate and severe winds.

Yearly development of errors in the wind fields

A further analysis on the wind fields was conducted at six locations, which included the five coastal locations and the Gloria offshore location. This was done to investigate whether or not the quality of the wind fields changed over the years. Yearly changes of two statistical error indicators (bias and SI) for all wind fields at the Kumköy, Hopa, and Gloria locations are shown in Figures. 7a-7c. In all wind fields at Kumköy, an improvement in the bias values appears to happen after the year 2002 in all data sources. However, there is a change in 2007 to 2010, where the error values increased. Another improvement is observed again in the year 2011 (Fig. 7a). The CFSR and MERRA winds have the highest error values in all years at this location, while the OPER and ERA-I have lower values. The ERA-I winds have the lowest errors in numerous years. At the Amasra location (not shown here), the scatter index values ranging between 50%-55% appeared in the ERA-I winds. In a case regarding the OPER winds, a scatter index value of 56% was available in 2004. Until 2007, this value constantly declined to 50% before increasing and reaching a maximum value of 58% in 2010. It is seen here that, in general, with average values of 2.53 m/s and 52% for the bias and SI, respectively, the ERA-I winds possessed the lowest error values at this location.

The MERRA wind fields yielded the highest error values at the Sinop location (not shown here) where a bias of 2.84 m/s for 2001 and an SI of 57% for the year 2010 were obtained. The OPER wind fields appear to have performed better (maximum bias = 1.46 m/s for 2001 and maximum SI = 0.48 for 2010) at all years. Higher error values (between 3.13-1.70 m/s for bias and 60%-84% for SI) were observed at the Giresun location (not shown here) for the OPER winds, especially over the years 2000 to 2006. Regardless of the error values of the ERA-I winds being relatively lower than in the OPER winds, the CFSR winds (0.43 m/s-1.20 m/s of bias and 43%-65% of SI) exhibited an overall best performance. Similar to at Giresun, the CFSR winds also performed very well at the Hopa location (Fig. 7b), while the OPER winds performed poorly here. The year 2006, in which all winds had the lowest error values, the CFSR winds (SI=56%)

Table 10. The statistical error values of all wind fields for the wind speed range between 8 m/s - 12 m/s for 2004-2007 for the coastal locations and 2006-2009 for the Gloria offshore location.

Location	Data Source	N	bias (m/s)	NMB	RMSE (m/s)	HH	MAE (m/s)	d	SI	r
Kumköy	CFSR	3505	2.30	-0.25	3.18	0.39	2.67	0.37	0.34	0.31
	MERRA	3505	2.18	-0.23	2.93	0.35	2.43	0.39	0.31	0.34
	ERA-I	637	0.16	-0.02	2.59	0.28	2.05	0.48	0.28	0.34
	OPER	637	0.26	-0.03	2.49	0.27	1.97	0.50	0.26	0.36
Amasra	CFSR	8016	4.82	-0.49	5.18	0.73	4.83	0.28	0.53	0.28
	ERA-I	1282	4.10	-0.42	4.65	0.61	4.19	0.31	0.47	0.27
	OPER	1282	4.27	-0.43	4.90	0.65	4.39	0.30	0.50	0.26
Sinop	CFSR	4970	3.26	-0.35	3.98	0.52	3.51	0.31	0.42	0.28
	MERRA	4970	4.19	-0.45	4.51	0.64	4.21	0.27	0.48	0.24
	ERA-I	884	2.99	-0.32	3.64	0.46	3.22	0.33	0.39	0.30
	OPER	884	1.85	-0.20	3.08	0.36	2.54	0.38	0.33	0.26
Giresun	CFSR	194	2.88	-0.31	3.77	0.49	3.29	0.22	0.41	0.08
	ERA-I	59	4.51	-0.50	4.77	0.74	4.51	0.17	0.52	-0.03
	OPER	59	5.82	-0.64	6.14	1.12	5.94	0.16	0.67	0.22
Hopa	CFSR	1284	4.74	-0.47	5.29	0.72	4.83	0.26	0.53	0.11
	ERA-I	419	6.57	-0.65	6.71	1.12	6.57	0.23	0.67	0.24
	OPER	419	7.13	-0.71	7.32	1.34	7.13	0.21	0.73	0.14
Gloria	CFSR	1147	0.34	-0.04	1.83	0.19	1.38	0.58	0.19	0.49
	MERRA	1147	1.70	-0.18	2.34	0.27	1.92	0.46	0.24	0.46
	ERA-I	1147	1.32	-0.14	2.02	0.23	1.58	0.53	0.21	0.52
	OPER	1147	1.17	-0.12	2.08	0.23	1.56	0.52	0.22	0.49

show a better performance compared to the other winds. The error-value margins in the other years were observed to be even wider apart. The annual changes of bias and SI determined by using Eqs. 2 and 3 for all wind fields at the Gloria offshore location are presented in Figure 7c. According to the measurements (Measurements-2) converted by using Eq. 3, the CFSR wind fields exhibited the best performance. For the other method (Measurements-1) the best performance was also obtained from the CFSR wind fields.

Conclusions and recommendations

Several statistical analyses were performed to assess the performances of four wind data sources in the Black Sea. The analyses were thus made using hindcast data sources' data sets against the measured data at five coastal locations on the southern shore of the Black Sea and an offshore location (Gloria) off the coast of Romania. The most important results can be summarized as follows, where each bullet contains a conclusion and a discussion of possible causes:

All data sources are negatively affected by orographic effects. This becomes worse toward the eastern part of the Black Sea. The CFSR winds perform best in comparison to the other data sources. This is due to the ability of the CFSR winds to capture sudden changes in the winds because of their higher temporal resolution (1 hour).

There is a clear geographical distinction in the quality of the wind fields. The ECMWF data sources could be suitable for applications in the western part of the Black Sea, whereas the CFSR winds can also be applicable for regional studies in the south eastern part of the Black Sea, where the orographic effect is much higher. The south eastern part of the Black Sea shows a worst performance of the wind fields because the spatial resolution of the digital terrain models is coarser compared to what is needed for a proper inclusion of the orographic effect. When the atmosphere is discretized into 0. 25° x 0. 25° (approximately 25 km x 25 km) cells, it is not possible to accurately represent the underlying atmospheric processes that generate the wind speeds. Therefore, a higher spatial resolution may be a solution for these problems.

The corrected measurements based on the wind profile power law in comparison with the profile log-law at Gloria show a more similar distribution to that of the data sources, except for the CFSR winds, which match well with the corrected measurements using Eq. 3.

The area-weighted interpolation method presents slightly better results than the distance-weighted method. The closest grid point to the measuring station sometimes provides better results but the results determined by interpolation are better in general.

Table 11. The statistical error values of all wind fields for the wind speed range greater than 12 m/s for 2004-2007 for the coastal locations and 2006-2009 for the Gloria offshore location.

Location	Data Source	N	bias (m/s)	NMB	RMSE (m/s)	HH	MAE (m/s)	d	SI	r
Kumköy	CFSR	279	3.83	-0.29	4.91	0.44	3.86	0.22	0.37	-0.18
	MERRA	279	3.89	-0.29	4.87	0.44	3.92	0.22	0.37	-0.24
	ERA-I	54	1.88	-0.14	4.06	0.33	3.04	0.16	0.31	-0.36
	OPER	54	1.88	-0.14	4.05	0.33	2.99	0.16	0.31	-0.34
Amasra	CFSR	3818	6.71	-0.47	7.00	0.68	6.72	0.30	0.50	0.51
	ERA-I	623	5.85	-0.42	6.24	0.58	5.89	0.32	0.44	0.45
	OPER	623	5.84	-0.42	6.35	0.59	5.87	0.32	0.45	0.47
Sinop	CFSR	738	4.57	-0.33	5.29	0.47	4.69	0.30	0.39	0.23
	MERRA	738	6.77	-0.50	7.07	0.73	6.77	0.24	0.52	0.16
	ERA-I	131	5.27	-0.38	6.20	0.58	5.30	0.26	0.45	-0.04
	OPER	131	4.03	-0.29	5.37	0.47	4.22	0.28	0.39	-0.08
Giresun	CFSR	26	21.60	-0.83	23.46	2.32	21.60	0.31	0.90	-0.61
	ERA-I	4	8.13	-0.56	8.64	0.90	8.13	0.31	0.60	-0.54
	OPER	4	10.82	-0.75	11.29	1.56	10.82	0.26	0.78	-0.39
Hopa	CFSR	267	6.62	-0.52	7.00	0.80	6.62	0.11	0.55	0.04
	ERA-I	97	8.96	-0.70	9.16	1.32	8.96	0.11	0.72	0.03
	OPER	97	9.47	-0.74	9.68	1.50	9.47	0.10	0.76	-0.03
Gloria	CFSR	183	0.25	-0.02	2.18	0.17	1.55	0.58	0.17	0.47
	MERRA	183	2.56	-0.20	3.24	0.28	2.59	0.38	0.25	0.40
	ERA-I	183	1.69	-0.13	2.74	0.23	1.89	0.44	0.21	0.42
	OPER	183	1.49	-0.12	2.55	0.21	1.72	0.50	0.20	0.47

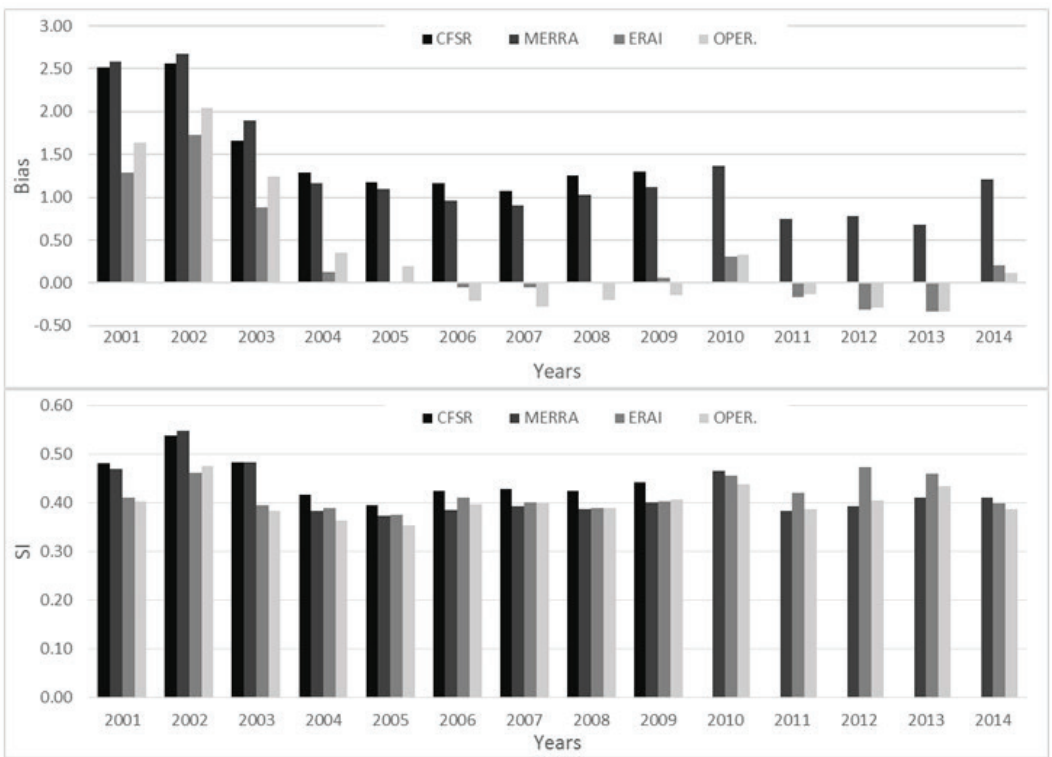

Fig. 7a: The yearly variation of the error statistics (as bias and SI) of the wind speeds at the Kumköy location.

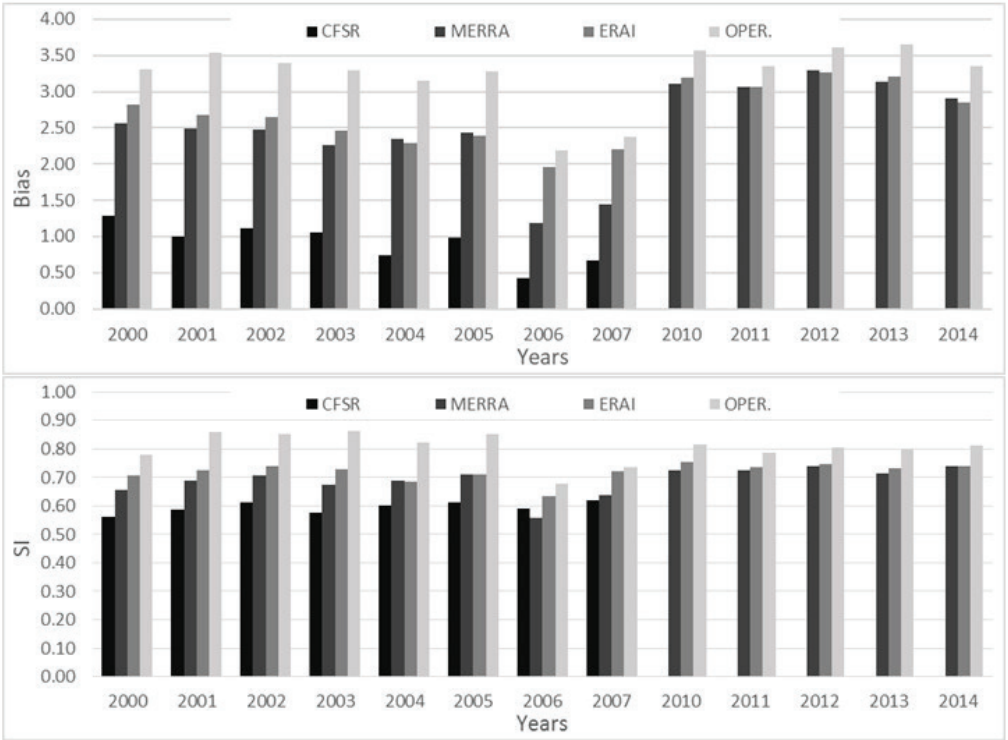

Fig. 7b: The yearly variation of the error statistics (as bias and SI) of the wind speeds at the Hopa location.

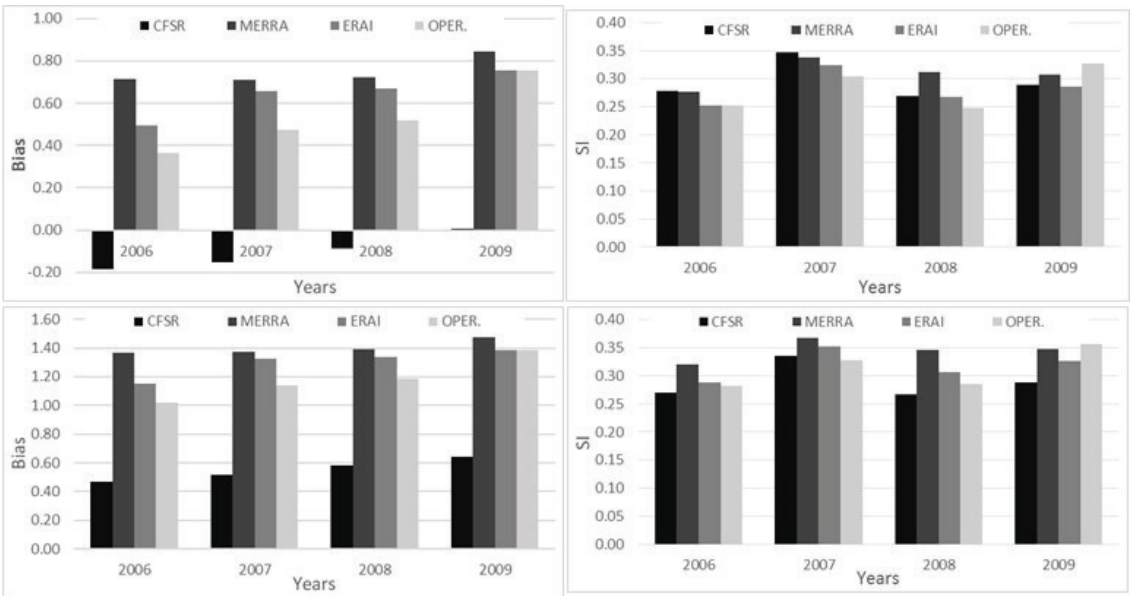

Fig. 7c: The yearly variation of the error statistics (as bias and SI) of the wind speeds at the Gloria location for Measurements-1 (upper) and Measurements-2 (bottom).

Along the southern coasts of the Black Sea, winds at higher speeds are often seen in the western regions in comparison with the ones in the east.

At all locations, the data sources perform better in predicting the direction of severe winds than predominant winds. Although all wind fields have a similar directional performance, the CFSR winds at the Gloria location have a better estimation ability than other data sources. All wind fields show a strong channeled flow in a dominant northeasterly direction at Kumköy, where they have some differences in comparison with the measurements due to missing orographic effects in the numerical atmospheric models.

The CFSR winds have a better performance in terms of bias and NMB at Gloria but the ECMWF winds also have a better quality in terms of some error indicators, such as RMSE, SI, and r. At this offshore location, all data sources have lower error and higher correlation values relative to the coastal locations.

The hindcast performance differs per wind field, per

wind speed range, per area, and per location. Along the southern coast of the Black Sea at Sinop and the western part of Sinop, the CFSR wind sources show better results at low speeds. At high speeds, despite the error values being high in this region, the ECMWF data sources have better performance. In the eastern part of Sinop, the CFSR winds perform better at high speeds than the other data sources. The CFSR winds at the Giresun location and the MERRA data sources at Hopa perform better at low speed ranges. At the Gloria offshore location, the ERA-I and CFSR winds perform well at low and moderate speeds, respectively. At high speed ranges, the CFSR wind fields appear to have the best performance.

In coastal locations, the yearly variation of error values of the data sources shows a variability in different years, with the highest errors in 2001. The yearly errors of the hindcasted wind speeds vary from year to year and there is no long-term trend of an increasing or decreasing error variation. This behavior, however, is not observed at the Giresun location. There are low variations in yearly error values (around SI = 30%) of the data sources at Gloria.

At all locations, the averages of the data sources are often below the measurement averages. All hindcast data sets are positively (right) skewed, which is consistent with the measurements. This is, accordingly, in relation to the intensity of the low speed values. The maximum values are well estimated at Sinop and western Sinop, contrary to eastern Sinop where these values are slightly lower.

At the Gloria location and in regions where the orographic impacts are low, the products of the re-analyses are usually in accordance with the measurements. On the other hand, it is understood that the reanalyses or the measurements may have a bias on the south eastern coast of the Black Sea, where the orographic effects are high. Therefore, it is recommended that a bias correction for the reanalyses (please see Staffell and Pfenninger, 2016) and the measurements (please see Azorin-Molina *et al.* 2018) should be checked to see if they are needed. For corrections of the model wind speeds, the satellite data, e.g., Quikscat might also be used.

Wind fields at the coastal areas are affected by the orographic structure. Therefore, a more accurate estimation of the near coastal winds can be conducted with a high-resolution regional wind prediction model.

Acknowledgements

This work is based on the master thesis of the first author at Uludağ University, Bursa, Turkey. We would like to thank the ECMWF, NCEP and NASA for providing the hindcast data sets, the NIMRD (Oceanography Department) for the providing the wind measurements at Gloria, and the TSMS for providing the wind measurements and for its assistance in recruiting the necessary permissions to obtain data from the ECMWF. The authors would like to acknowledge to Razvan Mateescu from the NIMRD Oceanography Department for helping in obtaining wind measurements recorded on the Gloria drilling platform. Finally, we thank the anonymous reviewers for their critical questions and suggestions, which improved our paper considerably.

References

Alvarez, I., Gomez-Gesteira, M., deCastro, M., Carvalho, D., 2014. Comparison of different wind products and buoy wind data with seasonality and inter annual climate variability in the southern Bay of Biscay (2000–2009). *Deep-Sea Research II*, 106, 38-48.

Ardhuin, F., Bertotti, L., Bidlot, J-R., Cavaleri, L., Filipetto, V. *et al.,* 2007. Comparison of wind and wave measurements and models in the Western Mediterranean Sea. *Ocean Engineering*, 34, 526-541.

Ardhuin, F., Roland, A., 2013. The development of spectral wave models: coastal and coupled aspects. p. 25-38. In: *Coastal Dynamics Conference '2013, Arcachon, 24-28 June 2013*. SHOM, France.

Arıkan, Ş.E., 1998. *Comparison of two different sources of wind data for wave prediction in the Black Sea*. MSc Thesis, Natural and Applied Sciences of METU, Ankara, Turkey, 227 pp. [in Turkish]

Azorin-Molina, C., Asin, J., McVicar, T.R., Minola, L., Lopez-Moreno, J.I. *et al.,* 2018. Evaluating anemometer drift: a statistical approach to correct biases in wind speed measurement. *Atmospheric Research*, 203, 175-188.

Barthelmie, R.J., Courtney, M.S., Højstrup, J., Larsen, S.E., 1996. Meteorological aspects of offshore wind energy: observations from the Vindeby wind farm. *Journal of Wind Engineering and Industrial Aerodynamics*, 62, 191-211.

Blackadar, A.K., 1960. A Survey of Wind Characteristics below 1500 ft. p. 3-11. In: *Topics in Engineering Meteorology-Meteorological Monographs*. American Meteorological Society, Boston, MA.

Caires, S., Sterl, A., Bidlot, J-R., Graham, N., Swail, V., 2004. Intercomparison of different wind-wave reanalysis. *Journal of Climate*, 17 (10), 1893-1913.

Carvalho, D., Rocha, A., Gomez-Gesteira, M., 2012. Ocean surface wind simulation forced by different reanalyses: Comparison with observed data along the Iberian Peninsula coast. *Ocean Modelling*, 56, 31-42.

Carvalho, D., Rocha, A., Gomez-Gesteira, M., Alvarez, I., Silva Santos, C., 2013. Comparison between CCMP, QuikSCAT and buoy winds along the Iberian Peninsula coast. *Remote Sensing of Environment*, 137, 173-183.

Carvalho, D., Rocha, A., Gomez-Gesteira, M., Silva Santos, C., 2014. WRF wind simulation and wind energy production estimates forced by different reanalyses: Comparison with observed data for Portugal. *Applied Energy*, 117, 116-126.

Cavaleri, L., Sclavo, M., 2006. The calibration of wind and wave model data in the Mediterranean Sea. *Coastal Engineering*, 53, 613-627.

Celik, A.N., 2002. Assessing the suitability of wind speed probability distribution functions based on wind power density. *Renewable Energy*, 28, 1563-1574.

Chelton, D.B., Freilich, M.H., 2005. Scatterometer-Based Assessment of 10-m Wind Analyses from the Operational EC-

MWF and NCEP Numerical Weather Prediction Models. *Monthly Weather Review*, 133, 409-429.

Cradden, L., Weywada, P.L., Atcheson, M., 2016. The offshore environment. p. 21-85. In: *Floating Offshore Wind Energy - Green Energy and Technology*. Cruz, J., Atcheson, M., (Eds). Springer International Publishing, Switzerland.

Davenport, A.G., 1965. The Relationship of Wind Structure to Wind Loading. p. 54-102. In: *National Physical Laboratory Symposium, Middlesex, 26-28 June 1965*. H.M. Stationery Office, London.

Dee, D.P., Uppala, S.M., Simmons, A.J., Berrisford, P., Poli, P. *et al.,* 2011. The ERA-Interim reanalysis: configuration and performance of the data assimilation system. *Quarterly Journal of the Royal Meteorological Society*, 137 (656), 553-597.

Dobson, F., Perrie, W., Toulany, B., 1989. On the deep water fetch laws for wind-generated surface gravity waves. *Atmosphere-Ocean*, 27, 210-236.

Hanna, S.R., Heinold, D.W., 1985. *Development and application of a simple method for evaluating air quality*. American Petroleum Institute, Health and Environmental Affairs Department, Washington, Technical report. 38 pp.

Hsu, S.A., 1980. On the correction of land-based wind measurements for oceanographic applications. p. 708-724. In: *17th Conference on Coastal Engineering*, *Sydney, 23-28 March 1980.* ASCE, Australia.

Jakobson, E., Vihma, T., Palo, T., Jakobson, L., Kernik, H. *et al.,* 2012. Validation of atmospheric reanalyses over the central Arctic Ocean. *Geophysical Research Letters*, 39, 1-6.

Jimenez, B., Moennich, K., Durante, F., 2012. Comparison between NCEP/NCAR and MERRA reanalysis data for long-term correction in wind energy assessment. In: *Europe's Premier Wind Energy Event (EWEA2012), Copenhagen, 16-19 April 2012.* EWEA, Denmark.

Lange, B., Larsen, S., Hojstrup, J., Barthelmie, R.J., 2004. Importance of thermal effects and sea surface roughness for offshore wind resource assessment. *Journal of Wind Engineering and Industrial Aerodynamics*, 92, 959-988.

Lileo, S., Petrik, O., 2011. Investigation on the use of NCEP/NCAR, MERRA and NCEP/CFSR reanalysis data in wind resource analysis. In: *Europe's Premier Wind Energy Event (EWEA2011), Brussels, 14-17 March 2011.* EWEA, Belgium.

Manwell, J.F., McGowan, J.G., Rogers, A.L., 2002. *Wind energy explained: theory, design and application*. John Wiley and Sons Ltd., West Sussex, UK, 705 pp.

Onea, F., Rusu, E., 2012. Evaluation of the wind energy resources in the Black Sea area. p. 26-32. In: *8th WSEAS International Conference on Energy, Environment, Ecosystems and Sustainable Development (EEESD'12), Faro, 2-4 May 2012.* Portugal.

Onea, F., Rusu, E., 2014a. An evaluation of the wind energy in the North-West of the Black Sea. *International Journal of Green Energy*, 11 (5), 465-487.

Onea, F., Rusu, E., 2014b. Wind energy assessments along the Black Sea basin. *Meteorological Applications*, 21, 316-329.

Onea, F., Raileanu, A., Rusu, E., 2016. Analysis of extreme wind and wave conditions in the Black Sea, as reflected by the altimeter measurements. *Mechanical Testing and Diagnosis*, 6 (1), 5-12.

Onea, F., Ciortan, S., Rusu, E., 2017. Assessment of the potential for developing combined wind-wave projects in the European nearshore. *Energy & Environment*, 28 (5-6), 580-597.

Onea, F., Rusu, E., 2018. Sustainability of the Reanalysis Databases in Predicting the Wind and Wave Power along the European Coasts. *Sustainability*, 10 (1), 193, 1-16.

Pimenta, F., Kempton, W., Garvine, R., 2008. Combining meteorological locations and satellite data to evaluate the offshore wind power resource of Southeastern Brazil. *Renewable Energy*, 33, 2375-2387.

Plate, E.J., 1971. *Aerodynamic characteristics of atmospheric boundary layer*, US Dept of Energy, Springfield, Virginia, 198 pp.

Ponce de León, S., Orfila, A., 2013. Numerical study of the marine breeze around Mallorca island. *Applied Ocean Research*, 40, 26-34.

Ragheb, M., 2017. *Wind shear, roughness classes, and turbine energy production*. University of Illinois, Lecture notes, 16 pp.

Rienecker, M.M., Suarez, M.J., Gelaro, R., Todling, R., Bacmeister, J. *et al.,* 2011. MERRA: NASA's modern-era retrospective analysis for research and applications. *Journal of Climate*, 24 (14), 3624-3648.

Saha, S., Moorthi, S., Pan, H-L., Wu, X., Wang, J. *et al.,* 2010. The NCEP Climate Forecast System Reanalysis. *Bulletin of the American Meteorological Society*, 91, 1015-1057.

Seguro, J.V., Lambert, T.W., 2000. Modern estimation of the parameters of the Weibull wind speed distribution for wind energy analysis. *Journal of Wind Engineering Industrial Aerodynamics*, 85, 75-84.

Sifnioti, D., Soukissian, T.H., Poulos, S., Nastos, P., Hatzaki, M., 2017. Evaluation of in-situ wind speed and wave height measurements against reanalysis data for the Greek Seas. *Mediterranean Marine Science*, 18 (3), 486-503.

Simmons, A., Uppala, S., Dee, D., Kobayashi, S., 2007. ERA-Interim: new ECMWF reanalysis products from 1989 onwards. *ECMWF Newsletter*, 110, 25-35.

Soukissian, T.H., Papadopoulos, A., 2015. Effects of different wind data sources in offshore wind power assessment. *Renewable Energy*, 77, 101-114.

Staffell, I., Pfenninger, S., 2016. Using bias-corrected reanalysis to simulate current and future wind power output. *Energy*, 114, 1224-1239.

Stanev, E.V., 2005. Understanding Black Sea dynamics. *Oceanography*, 18 (2), 56-75.

Stopa, J.E., Cheung, K.F., 2014. Intercomparison of wind and wave data from the ECMWF Reanalysis Interim and the NCEP Climate Forecast System Reanalysis. *Ocean Modelling*, 75, 65-83.

Strahler, A.H., Strahler, A.N., 1992. *Modern physical geography*. *4th Edition*. Wiley, New York, 320 pp.

Taylor, P.A., Lee, R.J., 1984. Simple guidelines for estimating wind speed variations due to small scale topographic features. *Climatological Bulletin*, 18 (2), 3-32.

US Army, 2003. *Coastal Engineering Manual, Chapter II-2 Meteorology and Wave Climate*, U.S. Government Printing Office, Washington (DC), USA, 77 pp.

Van Vledder, G., Akpınar, A., 2015. Wave model predictions in the Black Sea: Sensitivity to wind fields, *Applied Ocean*

Research, 53, 161-178.

Wang, A., Zeng, X., 2012. Evaluation of multireanalysis products with in situ observations over the Tibetan Plateau. *Journal of Geophysical Research*, 117, 1-12.

Willmott C.J., 1982. Some comments on the evaluation of model performance. *Bulletin American Meteorological Society*, 63 (11), 1309-1313.

Appendix A: Definitions of statistical parameters

To analyses the suitability of the hindcast data sets with the measurement data sets, the statistical parameters of the data sets themselves were determined. In coastal locations, the statistical parameters of the measurements and hindcast data sets were calculated for the overlapping four-year data between 2004 and 2007. At the Gloria location, a statistical evaluation was conducted using all data, since the available data was only taken over a period of four years and at a 6-hour interval. During the statistical analysis, measures of the central tendency of the data sets (arithmetic mean, mode, median, minimum and maximum values) were first determined. The distribution measures of the data sets were calculated following the computation of central tendency measures. The variance gives the average of the distance of each data to the mean of the data set. The standard deviation gives the averages of the distance of the data to the mean. Since the unit of the standard deviation is similar to that of the data, it shows the deviation more clearly than the average. The coefficient of variation indicating how much the standard deviation varies with the mean is given as:

$$CV = \frac{S}{\overline{X}} * 100 \tag{A.1}$$

One of the scatter metrics is the skewness coefficient which is another measure for data distribution and is calculated as below:

$$C_{sx} = \alpha_3 = \frac{m_3}{S^3} \tag{A.2}$$

where m_3 is the 3rd order moment relative to the average and is calculated as:

$$m_3 = \frac{\sum_{i=1}^{n} (X_i - \overline{X})^3}{n-1} \tag{A.3}$$

The data is left-skewed if the value is negative, right-skewed if positive and symmetrical if the value is zero. Finally, the excess Kurtosis parameter, which is a descriptor of the shape of a probability distribution and, just as for skewness, provides information about the peak of the probability distribution of the data sets. It was calculated as:

$$\alpha_4 = \frac{m_4}{S^4} - 3 \tag{A.4}$$

where m_4 is the 4th-order moment relative to the average and is calculated as:

$$m_4 = \frac{\sum_{i=1}^{n} (X_i - \overline{X})^4}{n-1} \tag{A.5}$$

Data with an excess kurtosis value of 0 is said to have a normal distribution. If this value is positive, the distribution has tails that asymptotically approach zero more slowly than a Gaussian distribution, and therefore produces more outliers (deviations) than a normal distribution. A negative excess kurtosis value means the distribution produces fewer and less extreme outliers than does the normal distribution.

Appendix B: Definitions of statistical error parameters

To properly judge the quality of any model it is recommended to apply a mixture of various statistical and graphical techniques, since using only one error criterion may lead to a misinterpretation of results. These criteria include several error indicators, such as the MAE, RMSE, bias, SI, etc., as well as the correlation coefficient and index of agreement. The first error value to be compared is the MAE, calculated as below.

$$MAE = \frac{1}{n} \sum_{i=1}^{n} | Y_i - X_i | \tag{B.1}$$

where Y_i are hindcast values, X_i are measurement values and n is the number of data points. Another error value is the RMSE, given by the equation below.

$$RMSE = \sqrt{\frac{1}{N} \sum_{i=1}^{n} (X_i - Y_i)^2} \tag{B.2}$$

Another error value, the average difference (bias), is calculated as:

$$Bias = \left(\overline{X} - \overline{Y} \right) \tag{B.3}$$

where is average of measurements and is the average of observations. To evaluate the performances of the wind speeds we used also the normalized bias NMB:

$$NMB = \frac{\sum \left(Y_i - X_i \right)}{\sum X_i} \tag{B.4}$$

The NMB shows the model tendency to over- or underestimate relative to the measurements. The index of agreement (d) introduced by Willmott (1982) was also used to make a cross-comparison between different models for the same observed dataset. This indicator varies from 0 to 1, with higher index values indicating that the modeled values have a better agreement with the observations.

$$d = 1 - \frac{\sum \left(Y_i - X_i \right)^2}{\sum \left(\left| Y_i - \overline{X} \right| + \left| X_i - \overline{X} \right| \right)^2} \tag{B.5}$$

The other indicator used for a cross-comparison between different models is the normalized root mean square error (HH) introduced by Hanna and Heinold (1985). The main advantage of this parameter is the fact that it is not biased toward simulations that underestimate the average and it is not sensitive to the mean observed values.

$$HH = \sqrt{\frac{\sum (Y_i - X_i)^2}{\sum Y_i X_i}} \tag{B.6}$$

After finding the error values, the SI values are calculated using the following formula:

$$SI = \frac{RMSE}{\overline{X}} \tag{B.7}$$

Finally, the correlation coefficient that shows the degree of correlation between measurements and hindcast data sets is calculated using the following equation.

$$r = \frac{\sum_{i=1}^{n} (X_i - \overline{X})(Y_i - \overline{Y})}{\sqrt{\sum_{i=1}^{n} (X_i - \overline{X})^2 \sum_{i=1}^{n} (Y_i - \overline{Y})^2}} \tag{B.8}$$

The correlation coefficient has a value between -1 and +1. The sign of the value shows the relationship direction and its value shows the strength. Absolute values that are close to 1 represent a strong linear relationship.